INVESTIGATION OF MECHANICAL PROPERTIES IN DYNAMIC SOLIDIFICATION USING CONFORMED COOLING TECHNIQUE

Author

Muhammad Ans

Registration Number

00000205469

Supervisor

Dr. Mushtaq Khan

DEPARTMENT OF DESIGN AND MANUFACTURING ENGINEERING

SCHOOL OF MECHANICAL & MANUFACTURING ENGINEERING

NATIONAL UNIVERSITY OF SCIENCES AND TECHNOLOGY

ISLAMABAD

JUNE, 2020

Effects of Dynamic Solidification on Properties of Die-Casted Alloys
Investigation of Mechanical Properties in Dynamic Solidification Using Conformed Cooling Technique

Author

Muhammad Ans

Registration Number

NUST2017MSDME205469

A thesis submitted in partial fulfillment of the requirements for the degree of

MS Design and Manufacturing Engineering

Thesis Supervisor:

Dr. Mushtaq khan

Thesis Supervisor's Signature:

_____

DEPARTMENT OF DESIGN AND MANUFACTURING ENGINEERING
SCHOOL OF MECHANICAL & MANUFACTURING ENGINEERING
NATIONAL UNIVERSITY OF SCIENCES AND TECHNOLOGY,
ISLAMABAD

June, 2020

THESIS ACCEPTANCE CERTIFICATE

Certified that final copy of MS / MPhil Thesis written by Mr. MUHAMMAD ANS, (NUST2017MSDME205469) of SMME has been vetted by undersigned, found complete in all respect as per NUST Statutes / Regulations, is free of plagiarism, errors and mistakes and is accepted as partial fulfillment for award of MS / M. Phil degree. It is further certified that necessary amendments as pointed out by GEC members of the scholar have also been incorporated in said thesis.

Signature: _____

Name of Supervisor: Dr. Mushtaq Khan

Date: _____

Signature (HOD): _____

Date: _____

Signature (Principal): _____

Date: _____

PLAGIARISM CERTIFICATE (TURNITIN REPORT)

This thesis has been checked for Plagiarism. Turnitin report endorsed by Supervisor is attached.

Signature of Student
Muhammad Ans

Registration Number
MS-DME-00000205469

Signature of Supervisor

DECLARATION

I certify that this research work titled "Investigation of mechanical properties in dynamic solidification using conformed cooling technique" is my own work. The work has not been presented elsewhere for assessment. The material that has been used from other sources it has been properly acknowledged / referred.

Signature of Student

Muhammad Ans

2017-NUST-MS-DME-205469

COPYRIGHT STATEMENT

ACKNOWLEDGEMENTS

ALLAH the Almighty deserve all the praise, who gave me the will, the courage and the health to accomplish this task. I would like to take this opportunity to express my sincere gratitude to my supervisor, Dr. Mushtaq Khan for his continued support and guidance during the entire course of my MS, without which I would not have been able to get so far.

My deepest thanks to my parents, whose persistent love, support and guidance remained a key of my entire life. Their prayers and involvement remained a driving force for all of my achievements in my life. I am thankful to Mr. Naveed Aslam who helped me in performing experiments. My sincere gratitude to my fellow colleague Mr. Haq Nawaz for his indefatigable support during course of my research.

I would also like to thank Dr. Najam ul Qadir, Dr Syed Hussain Imran and Engr. Abdul Mateen for being on my thesis guidance and evaluation committee.

At the end I pray for all those who help me in my effort.

Dedicated to my exceptional parents and adored siblings whose tremendous support and cooperation led me to this wonderful accomplishment.

ABSTRACT

Aluminum alloys are the most widely used alloys in the current era. Their applications range from high speed air crafts to domestic utensils. These are light weight but they are not as strong as steel. Many processes are used to increase their strength such as: addition of grain refiner, mechanical, ultrasonic or electromagnetic vibrations during solidification and squeeze casting. The purpose of this thesis is to propose a framework for eliminating or minimizing defects in casting process as well as increasing strength and hardness without performing separate heat treatment process. In this research mechanical vibrations are applied to the aluminum 2024 alloy in the range of 15Hz to 45Hz frequency and 0.5g to 1.5 acceleration at different pouring and die temperatures. Taguchi design of experiments approach was used to perform experiments and ANOVA was applied to get the results. Best results are obtained at 750°C pouring temperature, 150°C die temperature, 45Hz frequency and 1.0g acceleration which is then compared with the as-cast sample. It is observed that non-dendritic microstructure can be obtained by applying mechanical vibrations to the mould during solidification. The average grain size is reduced by 40.6%, hardness and ultimate tensile strength are improved by 13.5% and 10.6% respectively.

TABLE OF CONTENTS

CHAPTER 1 INTRODUCTION 8

1.1 Background and Motivation 8

1.2 Problem Statement 9

1.3 Objective 9

1.4 Scope 9

1.5 Research Methodology 9

CHAPTER 2 LITERATURE REVIEW 10

2.1 Introduction (Narrative Review) 10

2.2 Vibration During Solidification 10

2.3 Mechanical Vibrations 11

2.4 Work Already Carried Out on Dynamic Solidification 11

2.4.1 Mechanical Vibrations 11

2.4.2 Ultrasonic Vibrations and Squeeze Casting 13

2.5 Work already carried out on 2024 Aluminum alloy 14

2.5.1 Squeeze Casting 14

2.5.2 Modifier and Other Techniques 15

CHAPTER 3 MATERIALS AND METHOD 18

3.1 Methodology 18

3.2 Vibratory Table Setup 18

3.3 Sensors and Measurement Methods 19

3.4 Die Design 21

3.4.1 Mould 21

3.4.2 Heating System 22

3.4.3 Cooling System 22

3.5 Process Parameters 23

3.6 Material 25

3.7 Experimental Procedure 26
3.8 Heating and Cooling Curves of Mould 28
CHAPTER 4 TESTING AND SAMPLING 29
4.1 Tensile Test 29
4.2 Sample Preparation for Hardness and Optical Microscopy 30
4.3 Optical Microscopy 31
4.4 Hardness 32
CHAPTER 5 RESULTS AND DISCUSSION 33
5.1 Microstructure 33
5.2 Grain Size 35
5.3 Hardness 36
5.4 Ultimate Tensile Strength 37
5.5 ANOVA 38
5.5.1 Grain Size 39
5.5.2 Hardness 42
5.5.3 UTS 45
5.6 Confirmation Experiment and Comparison with As-Cast 48
5.7 Discussion 50
5.7.1 Grain Size 50
5.7.2 Hardness 51
5.7.3 Ultimate Tensile Strength 52
CHAPTER 6 CONCLUSIONS AND FUTURE WORKS 54
6.1 Conclusions 54
6.2 Future Works 55
CHAPTER 7 REFERENCES 56

LIST OF FIGURES

Figure 3-1: CAD Model of Vibratory Setup 18

Figure 3-2: Data Acquisition System 21

Figure 3-3: CAD model of Mould 21

Figure 3-4: (a) CAD Model of Mould with Heaters location, (b) Physical Mould with heaters (c) Heaters 22

Figure 3-5: (a) CAD model of cooling channels in die (b) Cooling Tank, (c) Complete Cooling Setup 23

Figure 3-6: Al-Cu Phase Diagram 26

Figure 3-7: (a) Melting in Furnace, (b) Die Pre-Heating, (c) Pouring from Crucible to Pouring Cup, (d) Pouring through Pouring Cup, (e) Vibration On, (f) Vibration Stopped and Holding, (g) Water Pump on for Cooling, (h) Steam Out, (i) Casted Parts 27

Figure 4-1: (a) Tensile test sample dimensions, (b) Physical Samples 29

Figure 4-2: Universal Testing Machine 29

Figure 4-3: Mounting Machine 30

Figure 4-4: Manual Grinding Machine 30

Figure 4-5: Automatic Polishing Machine 31

Figure 4-6: Optical Microscope 32

Figure 4-7: Micro Vicker Hardness Testing Machine 32

Figure 5-1: Micrographs of Run 1 to Run 9 samples from Top and Bottom sides 35

Figure 5-2: Optical Micrographs of (a) Top Side, (b) Bottom Side of Confirmation Experiment, (c) Top Side, (d) Bottom Side of As-cast 49

LIST OF TABLES

Table 3-1: Vibratory Setup Operating Range 19

Table 3-2: Thermocouple Specifications 21

Table 3-3: Heater Specifications 22

Table 3-4: Heating Temperature vs Time 22

Table 3-5: Cooling System Specifications 23

Table 3-6: Input Parameters and Levels 23

Table 3-7: L9 Orthogonal Array 24

Table 3-8: Orthogonal Array with Real Values 25

Table 3-9: Al-2024 Alloy Composition 26

Table 5-1: Grain Size Results 35

Table 5-2: Hardness Results 36

Table 5-3: UTS Results 37

Table 5-4: Signal to Noise Ratio for Grain Size 39

Table 5-5: Contribution, F and P Values for Grain Size 40

Table 5-6: Delta and Rank for Grain Size 40

Table 5-7: Signal to Noise ratio for Hardness 42

Table 5-8: Contribution, F and P Values for Hardness 43

Table 5-9: Delta and Rank for Hardness 43

Table 5-10: Signal to Noise Ratio for UTS 45

Table 5-11: Contribution, F and P Values for UTS 46

Table 5-12: Delta and Rank for UTS 46

Table 5-13: Optimum Parameter Values 49

Table 5-14: Results of Confirmation Experiment and As-cast 50

LIST OF GRAPHS

Graph 3-1: Heating and cooling temperature curves at different die temperatures 28

Graph 5-1: Average Grain Size vs Runs 36

Graph 5-2: Average Hardness vs Runs 37

Graph 5-3: Average UTS vs Runs 38

Graph 5-4: Graph of SN ratios for Grain Size 41

Graph 5-5: Graph of Means for Grain Size 41

Graph 5-6: Graph of SN ratios for Hardness 44

Graph 5-7: Graph of Means for Hardness 44

Graph 5-8: Graph of SN ratios for UTS 47

Graph 5-9: Graph of Means for UTS 47

Graph 5-10: Graph of Means for Combined effect of hardness and UTS 48

Graph 5-11: Comparison of Grain Size, Hardness and UTS of Optimum and As-Cast Experiments 50

CHAPTER 1
INTRODUCTION

1.1 **Background and Motivation**

Aluminum alloys are the most commonly used casting alloys. They are used for wide range of applications from kitchen utensils to the air craft body. They especially used in transport filed due to their high strength to weight ratio, good corrosion resistance, and excellent castability. Automotive industry is using aluminum parts instead of iron to reduce the weight of the cars, for example, pistons, engine blocks, cylinder heads to improve fuel efficiency.

Although aluminum alloys do not belong to the latest breakthrough materials but they are widely used alloys all over the world. Parts made from classic casting aluminum alloys has probably reached its top and no upcoming casting technologies are producing parts with improved mechanical properties. So, there is a time came to use wrought aluminum alloys in casting applications to get benefit of their properties. Wrought aluminum alloys show superior properties as compared to casting aluminum alloy. So, they have wide applications in automotive and aerospace industry. Wrought aluminum alloys were mainly used in processes which include plastic deformation such as extrusion forging and rolling which increases the cost of manufacturing. But now a days wrought aluminum alloys are also being used in casting of near net shape and higher shape complexity parts which reduces the cost of manufacturing. The research of all unconventional technologies such as casting with crystallization pressure or semi-solid metals casting has already been engaged. The problems occur during casting of these alloys are they have low fluidity and long solidification range that causes defects like hot tearing, porosity, shrinkage, and formation of dendrites.

Using copper as a main alloying element, aluminum alloys of 2xxx series, for example 2024 aluminum alloy, etc., are very attractive material due to their excellent properties such as good formability, age hardenability and strength to weight ratio, they are widely used in automotive and aerospace industry. However, aluminum alloys show deficiencies in mechanical properties which arises from casting defects and inappropriate microstructure. The mechanical properties of the cast component strongly depend on the microstructure which in turn depends on the chemical composition and solidification conditions provided by the casting system such as mould, cooling circuit, coolers, cores etc.

Microstructure can be refined either by chemical method in which nano particles are added to the melt to refine the microstructure, or my mechanical method in which pressure or vibrations

are applied to the melt. Various types of vibrations are; mechanical vibrations, ultrasonic vibrations and electromagnetic vibrations. To obtain refined microstructure, applying mechanical vibrations to the mould during solidification is an advantageous method because of low cost and simple system as compared to ultrasonic and electromagnetic vibrations.

1.2 **Problem Statement**

Today Industry need high strength and lightweight materials, aluminum alloys could be one of these materials but their mechanical properties are no so good to replace steel, so there is a need to improve mechanical properties of aluminum alloys. The attempt is made to improve mechanical properties of wrought Aluminum 2024 alloy.

1.3 **Objective**

The main objective of this thesis is to study the effects of mechanical mould vibration on the microstructure and mechanical properties of die-cast aluminum 2024 alloy. The final goal consists in the improvement of the mechanical properties such as hardness and ultimate tensile strength of castings and at this purpose a non-dendritic and refined microstructure is preferable.

1.4 **Scope**

The scope of this thesis is to made parts out of casting using vibration in the mold during solidification by changing different parameters like frequency, heating temp, etc.

1.5 **Research Methodology**

In this thesis experiments are performed according to Taguchi Design of Experiments approach to minimize no of experiments.

The thesis is structured as following:

Chapter I	Introduction
Chapter II	Literature Review
Chapter III	Material and Methods
Chapter IV	Sampling and Testing
Chapter V	Results and Discussion
Chapter VI	Conclusion & Future Works
Chapter VII	References

CHAPTER 2
LITERATURE REVIEW

2.1 **Introduction (Narrative Review)**

Microstructure of a casting is a main factor that affects mechanical properties of aluminum alloys. Refining the microstructure to achieve fine and equiaxed grains will reduce micro porosity, reduce hot cracking and increase fluidity. In hypoeutectic alloys if the solidification is well grain refined, the casting will have non-dendritic microstructure. For minimizing segregation problems and porosity and for obtaining globular structures, semi solid processing is the best process. In the semi solid processing a specific shear is required which is given from external sources because SSM billets have thixotropic characteristic that is when the stress is low, they will have high viscosity but when stress is increased, they show low viscosity. Different techniques that are used to improve mechanical properties of alloys during casting are; mechanical vibrations, ultrasonic vibrations, electromagnetic vibrations, squeeze casting, and addition of grain refiner and rapid cooling.[1]

In the last two decades, it was found that improvement in mechanical properties can be achieved by the method of adding nano particles into the melt of an alloy. Several publishers have pointed out that by the addition of nanoparticles of TiC, TiB, AlO and WC during casting process can improve mechanical properties of A356 alloy.[2]

Literature related to above mentioned processes is collected for this thesis.

2.2 **Vibration During Solidification**

The effects of dynamic solidification have been in the literature since 1868 but it was not clarified due to different methods, materials, and a non-systematic approach that were used to perform these experiments. Dynamic condition can be applied in two ways: first one is to apply vibrations to the mould either in vertical axis or in horizontal axis, second type is to vibrate only the melt before solidification. For the latter, electromagnetic fields or melt able vibrating probes can be used either in cooled or uncooled condition but they show technological disadvantages. The frequency and amplitude that were used by different authors lies in the range of as low as 1Hz-1cm mechanical vibration to as high as 3000Hz-10um ultrasonic vibrations. Most of the authors used steel, cast iron or graphite mould. [3]

2.3 **Mechanical Vibrations**

From the techniques described in the previous section applying mechanical vibrations to the mould is an advantageous method to get fine microstructure as compared to ultrasonic or electromagnetic vibrations due to its simple system and low cost. The mechanical vibrations can be further classified in two types. In the first type, mechanical vibrations are applied to the mould in the continuous cooling melt. It has been shown that vibrations had strongly affected the cast billets, such as refinement of grains, improvement in mechanical properties and degassing. In the second type, mechanical vibrations are applied to mould at various solid fractions of the molten alloy in the mushy zone i-e between solidus and liquidus temperature.it has been revealed that mould has absorbed the energy which was produced from latent heat and superheat of molten alloy. Introducing mechanical vibration during casting improves macro- and microstructures, good surface finish and reduced porosity and shrinkage defects.[4]

In the literature studied authors investigated the effects of ultrasonic vibrations during solidification and squeeze casting on Aluminum 2024 alloy but no one has studied the effects of mechanical vibrations. So, in this research an experimental approach is used to study the effects of mechanical mould vibrations during solidification of the continuous cooling casting of Aluminum 2024 alloy. This method was not widely used up to now due to expensive equipment and size limitation. The new development of dynamic system technology, with low investment, could permit new interesting largescale industrial applications.

2.4 **Work Already Carried Out on Dynamic Solidification**

2.4.1 **Mechanical Vibrations**

Limmaneevichitr et al.[1] investigated the influence of mechanical vibration on macrostructure and microstructure of Aluminum A356 alloy during solidification at different pouring temperatures and solid fractions. It was found that at the lower pouring temperature of 630°C and higher solid fraction of 40%, the normal dendrites were fragmented and disturbed and the primary aluminum phase became globular and finer.

Konstantin et al.[2] compared the effects of mechanical vibration and addition of modifier on density and mechanical properties of Al-Si casting alloy. Results revealed that by applying vibrations of 100Hz without modifier showed best properties as tensile strength was increased by 20% and yield strength was increased by 10%.

Appendino et al [3] investigated the effects of mechanical vibration on the microstructure and mechanical properties on sand casting of aluminum A356 alloy. They concluded that the use of higher acceleration caused a non-dendritic and globular microstructure. The highest UTS was obtained at acceleration of 3g with high amplitude.

Guo et al. [4] studied effects of mechanical vibration treatment before pouring on Al−5%Cu aluminum alloy using melt able vibrating probe. They found that by increasing vibration acceleration improves microstructure, coarse dendrites were converted into fine and uniform ones and a non-dendritic microstructure was obtained. Best results were obtained at vibration acceleration of 19m/sec^2 with an average grain size of 61um which was decreased from 343um when the acceleration was 2.5m/sec^2.

Chaturvedi et al. [5] studied effects of mechanical vibration on structure and properties of Mg-9Al alloy during solidification. It was concluded that on increasing the frequency from 31Hz to 40Hz of mechanical vibration during solidification refines microstructure and improves tensile strength and hardness.

Mishra et al.[6] investigated the influence of mould vibration on microstructure and mechanical properties of Al-6wt.%Cu alloys during casting at different frequencies from 40 to 120Hz. It was found that the grain structure was refined with the application of mechanical vibrations. They concluded that hardness and wear resistance were improved with the increase in frequency. However, UTS was reduced with the increase in vibration frequency.

Fatai et al. [7] studied the effects of mechanical vibration on hardness, impact and tensile strength during solidification of AZ91 magnesium alloy. The tests were conducted in the frequency range of 4-24Hz. They found that mechanical properties were improved up to 16Hz frequency and then decreases with further increase in frequency. They concluded that vibration caused refinement of microstructure and best mechanical properties were found in the frequency range of 12Hz to 16Hz.

Chen et al. [8] studied the influence of mechanical vibration on microstructure, tensile strength and solidification filling of cast AZ91D magnesium alloy. They applied vibrations in the range of 35-150Hz frequency and 0.2-1.0mm amplitude. They concluded that when frequency was 100Hz and amplitude was 1.0mm, maximum mould filling and tensile strength were achieved.

Silva et al. [9] investigated the influence of mechanical vibration on tensile strength and solidification behavior of an Al–18wt.%Si alloy. Mechanical vibrations were applied at 8 and

24Hz frequency. They concluded that at the vibration frequency of 8Hz, maximum rapture strength and rapture strain were obtained.

Abhilash et al. [10] compared the influence of mechanical vibration on porosity and α-aluminum dendritic morphology in cast A356 aluminum alloy solidified under furnace cooling (600°C to 35°C) and air cooling (35°C) atmosphere. They found that effect of vibration on Secondary Dendritic Arm Spacing is much significant in air cooling compared to furnace cooling.

Gencalp et al. [11] compared the effects of mechanical vibration on gravity casting and cooling slope casting to an $AlSi_8Cu_3Fe$ alloy at 5.75Hz frequency. They found that α-Aluminum particles were more spherical in cooling slope casting under vibration as compared to gravity casting under vibration and cooling slope casting without vibration. They also concluded that low frequency is more suitable for cooling slope casting than for gravity casting. To achieve the same results from gravity casting, frequency must be increased.

Khmeleva et al. [12] studied different types of casting experiments on A356 Aluminum alloy: by applying vibration treatment on A356 alloy, using Al-TiB_2 composite master alloy and by applying vibrations on Al-TiB_2 composite master alloy. It was found that by applying mechanical vibration to Al-TiB_2 composite master alloy gave best results. Average grain size was reduced to 140um and tensile strength was increased to 227 MPa.

Fan et al. [13] applied mechanical vibrations to the solidification of A356 aluminum alloy made by investment casting to study the effects of different peak accelerations on the mechanical properties of the casted parts. When the peak acceleration was between 1 and 4 g, the primary α-Al grains were refined significantly, secondary dendrite arms were broken, the average grain size was reduced, and the alloy's mechanical properties increased notably. When the peak acceleration was greater than 4 g, strong vibrations lead to defects formation such as sand adhesion, and the migrating, gathering and growing of the bubbles, which lead to the formation and growth of pores.

2.4.2 **Ultrasonic Vibrations and Squeeze Casting**

Sahadeva et al. [14] studied the effects of ultrasonic treatment on microstructure and mechanical properties of Al-5Ti-1B/A-356 aluminum alloy during solidification. It was seen that for hardness 0.4wt% of grain refiner, 28KHz frequency ,0.08mm amplitude and 80sec of vibration holding time was more effective and for ultimate tensile strength 0.8wt% of grain

refiner, 20KHz frequency, 0.08mm amplitude, and 80sec of vibration holding time gave best results. That was due to cavitation that assist fragmentation to produce small grain size which increased tensile strength.

Kishor et al. [15] investigated the influence of ultrasonic vibrations on grain structure and mechanical properties during solidification of pure aluminum casting. It was found that microhardness was increased from 42.8Hv to 48.21Hv and ultimate tensile stress from 36.11 MPa to 68.01 MPa when using ultrasonic vibration.

Zhang et al. [16] investigated the combined effect of applied pressure and ultrasonic vibration on microstructure and mechanical properties of Al-5.0Cu-0.6Mn-0.6Fe aluminum alloy. The best tensile properties produced by P and UT processing were; UTS: 268MPa, YS: 192MPa, E.L.: 17.1%, respectively, which increased by 64%, 59% and 307%, respectively, compared to the non-treated alloy.

Manoj et al. [17] had investigated effects of squeeze casting on Al-SiC metal matrix composite. Fine grain structure and improved mechanical properties were obtained by applying pressure during solidification as compared to without pressure.

2.5 **Work already carried out on 2024 Aluminum alloy**

2.5.1 Squeeze Casting

Marashi et al. [18] studied the effects of high pressure casting of AA2024 aluminum alloy on yield stress, hardness, porosity and microstructure. It was observed that best results observed at lowest pouring temperature of 700°C and highest pressure of 140MPa. The yield stress was from 235MPa to 340 MPa and hardness was increased from 125HBN to 152HBN, dendritic arm spacing was reduced to 12.5um and porosity diameters were reduced to 0.25um and due to lower porosity density was increased from 2.19g/cm^3 to 2.75 g/cm^3 and an average grain diameter of 0.08um was observed. It was also noted that at squeezing pressures higher than 70MPa, the effects of pouring temperature were not significant

Hajjari et al. [19] compared the tensile properties, microstructure and density of squeeze casting and gravity die casting of wrought Aluminum 2024 alloy. The effects of pressure on the tensile strength and microstructure of alloy were studied in this research. They concluded that up to squeeze pressure of 50MPa, the tensile properties were improved due to high density which was caused by the elimination of the porosities. However, above 50MPa pressure, higher cooling rates caused microstructure to be finer which increased tensile properties.

Dhanashekar et al. [20] overviewed the squeeze casting of the aluminum metal matrix composites. It was concluded that in the squeeze casting of aluminum alloys and composites, the pressure of 100MPa can provide refined microstructure and improved mechanical properties. They suggested that pouring temperature between 600°C and 700°C and die temperature near 250°C gives better results during the squeeze casting of aluminum alloys and composites.

Vanko et al. [21] studied the effects of squeeze casting on EN AW-2024 wrought aluminum alloy. The samples casted at lower pouring temperature of 650°C showed non-dendritic microstructure and the samples casted at higher pouring temperature of 700°C showed dendritic microstructure. But after heat treatment, the sample which was casted at 700°C and had dendritic microstructure, showed highest mechanical properties

Yuandong et al. [22] studied the influence of rheo-diecasting on solidification behavior and microstructure characteristics of wrought aluminum 2024 alloy with self-inoculation method. Results showed that high-quality semi-solid slurry with fine and uniform primary α -Al grains can be produced from self-inoculation method in rheo-diecasting. The primary α -Al phase particles are those with non-entrapped liquid. The average equivalent diameter of grains was 70.80 μm and 74.15 μm, the shape factor is 1.32, and 1.42 after the semi-solid slurry was isothermally held at 625 ℃ for 3 min and 5 min, respectively.

Chen et al. [23] compared the mechanical properties of ultrasonic assisted squeeze casting and conventional squeeze casting of a wrought aluminum 2024 alloy. They found that by increasing ultrasonic power from 0 to 1.8kW, the microstructure was refined and coarse dendrites were converted into fine and equiaxed grains. At 1.8kW ultrasonic power, the ultimate tensile strength was increased by 20.8%, yield strength was increased by 21.2% and %elongation was improved by 84.8%, as compared to conventional squeeze casted part.

2.5.2 Modifier and Other Techniques

Qiang et al. [24] studied the influence of solution treatment and subsequent aging on the UTS, hardness and microstructure of Al_3Ti/2024Al composites with different amount of grain refining particles, produced by ultrasonic vibrations and squeeze casting. Results showed that with mass fractions of grain refiner between 4wt.% and 16wt.%, solution treatment at 500°C for 6hrs holding was suitable for in-situ Al_3Ti/2024 Al composites. The peak hardness was increased by 20.3% as the reinforcement particles were increased from 0% to 16%. Tensile and compression strengths had also increased gradually with the increase of grain refiner.

Leng et al. [25] studied the effects on mechanical properties by adding graphite particles into SiC/Al composites made by squeeze casting technology. Results showed that graphite particles had a negative effect on properties as the volume percentage and grain size of particles was increased. At 5vol.% of graphite particles, by increasing particle size from 1um to 70 μm, the tensile strength was decreased from 420MPa to 235MPa and modulus of elasticity was dreased from 166GPa to 116GPa

Krzysztof et al. [26] studied the influence on microstructure, tensile strength and wear resistance of C/Al_2O_3/2024 Aluminum alloy composites. Tensile and bending tests were performed in the temperature range between 20 and 300°C. Results showed that reinforcement with 10-20% fibers on aluminum matrix improved mechanical properties as compared to the unreinforced alloy. The highest increase in properties was occurred when the mechanical properties were measured at 300°C. replacing Al_2O_3 saffil fibers with carbon fibers had only increased wear resistance with no significant effect on tensile and bending properties.

Rao et al. [27] investigated the influence of applied pressure on wear resistance of SiC/2024 aluminum alloy with different weight percentages of SiC particles under varying seizure pressure. Results showed that when 10wt.%SiC particles were added to 2024 alloy matrix, the wear resistance was increased by 33% and when 25wt.%SiC particles were added, the wear resistance was increased by 50% as compared to the unreinforced alloy. Seizure pressure was not significantly affected between 10-15% of SiC particles.

Zhao et al. [28] investigated the effects of ultrasonic vibrations with different sonication time on the microstructure and tensile properties of ZrB_2/2024 aluminum alloy composites. Results showed that with the sonication time of 5 minutes and 10vol.% of ZrB_2 particles, few defects and improved mechanical properties were obtained. Tensile strength, yield strength, and %elongation was increased by 21%, 77% and 10% as compared to the composite without ultrasonic treatment, respectively.

Li et al. [29] investigated the effects of pouring temperature, electromagnetic vibrations and thixoforming during casting of 2024 aluminum alloy. Results showed that pouring temperature of 660°C, magnetic pules frequency of 6Hz, reheating temperature of 620°C and holding time of 30 minutes were optimum. They found that with decreasing pouring temperature and increasing magnetic pulse frequency to a certain level, the α-aluminum particles became rounder and much finer, however further increasing pulse frequency caused coarse microstructure again.

Guo et al. [30] examined the influence of different processing conditions on the microstructure of semi-solid slurries of wrought aluminum 2024, 6082 and 7075 alloys prepared by the LSPSF (low superheat pouring with a shear field) rheo-casting process. Experimental results showed that rheo-forging based on LSPSF process produced relatively homogenous grain structure. Metal flow was promoted and resulted in liquid/solid segregation in the high solid fraction of semi-solid slurry. Mechanical properties were improved with subsequent heat treatments.

CHAPTER 3
MATERIALS AND METHOD

3.1 **Methodology**

Experimental procedure was used to study the effects of mechanical vibration during solidification of Aluminum 2024 alloy. Vibratory table and mould were designed and manufactured according to specifications. Permanent mould was used which had heating and cooling channels for controlling cooling rate. Samples were made using vibration and one sample without vibration was also produced for comparison of mechanical properties.

3.2 **Vibratory Table Setup**

A vibratory table was designed and manufactured for the generation of required vibrations. The table consisted of following; base table, motor, VFD, springs, attachments for sensor and holding jags of mold. The working part of table consisted of flat plate of steel with attachments to hold the motor at bottom and mould attachment at top. Motor fastened upside down with the help of bolts. Motor was attached horizontally (x-axis) parallel to the ground so that vibration could be produced in vertical direction (z-axis). The upward surface of Steel Sheet was horizontally flat and carried permanent mould on it within the welded jags. 4x springs were attached as damper as well as to maintain unidirectional vibration. The lower part of table consisted on legs to keep the complete table rigid and firm. The overall length of springs was 170mm. Cad model of the vibratory table is shown in figure below.

Figure 3-1: CAD Model of Vibratory Setup

The table contained a three phase AC motor having 2850 rated rpms. Eccentric weights were attached to the motor's shaft according to the required amplitude of vibration. A Variable Frequency Drive (VFD) was attached to the motor for controlling frequency of the motor. The overall processing range of the system is summarized in table below.

Table 3-1: Vibratory Setup Operating Range

Parameter	**Range**
Frequency	0-47 Hz
Acceleration	0-20 m/sec
Amplitude	0-2 mm
Load	22 kg

3.3 **Sensors and Measurement Methods**

A specially made electronic circuit was used to measure acceleration of vibration. It consisted of IMU sensor (MPU 6050), Arduino Mega and jumper wires. Sensor gave its readings to Arduino and Arduino then displayed these readings on monitor screen using the Arduino software.

For frequency measurement, a VFD was attached to the motor which converts single phase AC to three phase AC and changes motor's speed by varying frequency of the current. VFD intakes single phase, 50 Hz and 220 Volts AC supply and then then send it to motor with three phase AC with varied current frequency. Frequency of current was varied through a knob on VFD which ultimately varied motor's speed. Vibration frequency was measured directly with the help of tachometer which measures rpms of motor. As the Motor speed at 220 V AC is 2850 RPMs so the formula to calculate the frequency is as follow:

$$\text{frequency(f)} = \text{rpms of motor}/60 \quad \text{……..…….3.1}$$

So, for 2850 rpms, frequency is equal to 47.5 Hz

The vibration amplitude which is the characteristic which describes the severity of the vibration is the peak to peak value from the static position of table. Vibration Amplitude was measured directly with the help of dial indicator.

Another parameter of vibration was measured in terms of the acceleration which is calculated in "*g*" (1g is equals to 9.8 m/sec^2). The vibration amplitude is a quantification of acceleration in term of g. Value of acceleration that is '*g*' was varied by using three different eccentric weights. The value of 'g' for an eccentric weight is calculated as follows:

$$F_c = m_e r w^2 \quad \text{……..……...……...……3.2}$$

Where F_c is called centripetal force, m_e is the mass of eccentric rotating semi-circle, r is the radius of center of mass for eccentric rotating mass calculated by $4r/3\pi$, and ω is angular frequency which is equal to $2\pi f$.

$$F_g = m_o g \quad \text{…….……....…….……...……3.3}$$

Whereas F_g is force due to gravitational potential energy, m_o is overall mass of the vibrating part and g is the acceleration. In case of eccentric rotating mass.

$$F_c = F_g \quad \text{……..……..…….…3.4}$$

By comparing Eq. 3.3 and 3.4

$$m_o g = m_e r w^2 \quad \text{……..……3.5}$$

$$g = m_e r w^2 / m_o \quad \text{……...……...…….…..……3.6}$$

Calculated values are approximately closed to measured value of sensor system this calculation helps to design & manufacturing of the eccentric rotating mass for generation of required gravitational acceleration.

For temperature readings, two k-type thermocouples, Max6675 IC, Arduino Mega and jumper wires. Thermocouples are fitted in the die at different locations. These thermocouples are connected to MAX-6675 IC which functions as cold-junction compensation and converts the signal into digital form which was sent from a type-K thermocouple. The Temperature was translated to a directly proportional voltage and the relation was linear over the concerned operating range. The data is output in a 12-bit resolution. The MAX- 6675 sends digital signal to the Arduino so that the Arduino can read it, store it and display it on a monitor screen using Arduino software.

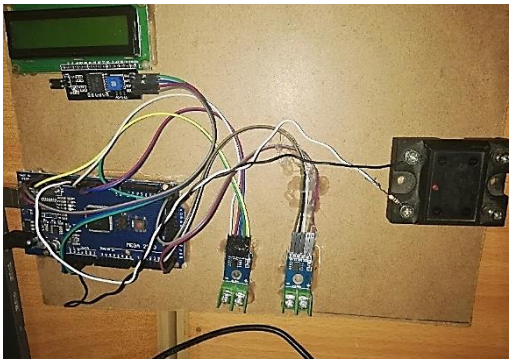

Figure 3-2: Data Acquisition System

Table 3-2: Thermocouple Specifications

Sensor	Type	Range	Size (Día)	Form
Thermocouple	K-Type	0-800°C	3/8 inches	Stud-type

3.4 **Die Design**

As the setup is vibratory so sand mould was difficult to use because it can collapse at heavy vibrations, for that reason permanent mould made of mild steel was used in this research. The die contained the following; mould cavity for casting, four cartridge heaters for maintaining die temperature and water channels for cooling.

3.4.1 **Mould**

A round cylindrical shaped mould cavity was made in the die. The molten metal was poured in the mould from the top. Its diameter and length are 35mm and 115mm respectively. The cad model of die is shown in figure below.

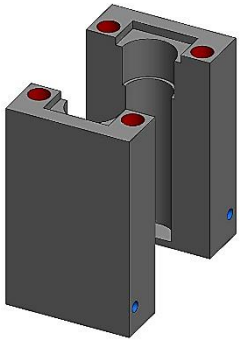

Figure 3-3: CAD model of Mould

3.4.2 **Heating System**

4x cartridge heaters were used to preheat the die and maintained at that temperature for 10 minutes after pouring using Arduino and relay system. Physical heaters and Cad model of their location in die are shown in figure below.

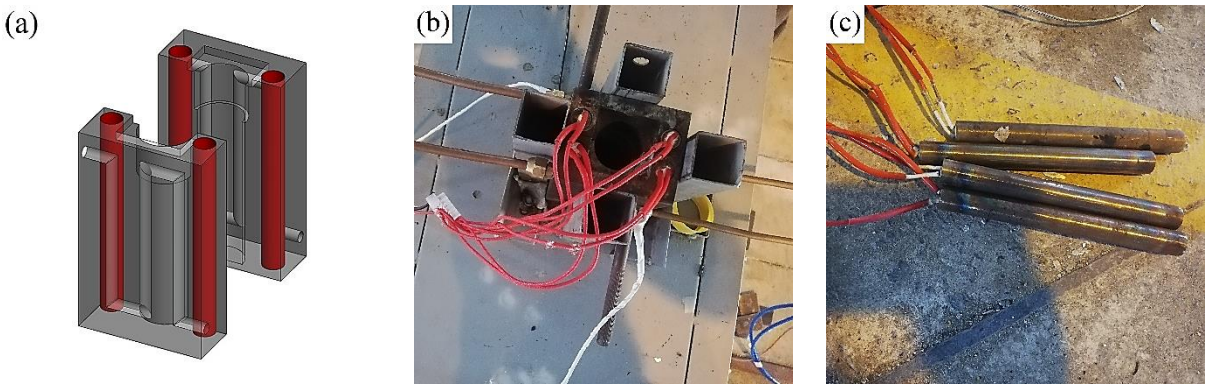

Figure 3-4: (a) CAD Model of Mould with Heaters location, (b) Physical Mould with heaters (c) Heaters

Heater specifications are given in table below.

Table 3-3: Heater Specifications

Parameter	**Power**	**Length**	**Diameter**	**Power Supply**	**Maximum Temp**
Value	600 Watts	145 mm	16 mm	220 V AC	560°C

Time taken by the heaters to heat the die up to required temperatures is shown in table below.

Table 3-4: Heating Temperature vs Time

Temp (°C)	150	300	450
Time (min)	8.5	17.75	33.5

3.4.3 **Cooling System**

Water channels were made in both parts of the die. Water entered the die at top left corner and left the die at right bottom corner. A water tank was placed near the setup for water supply. Water pump was placed in water tank which supplied fresh water. Pump and die were connected by flexible pipes Water at outlet was drained off using pipes. Cad Model and physical cooling system are shown in figure below.

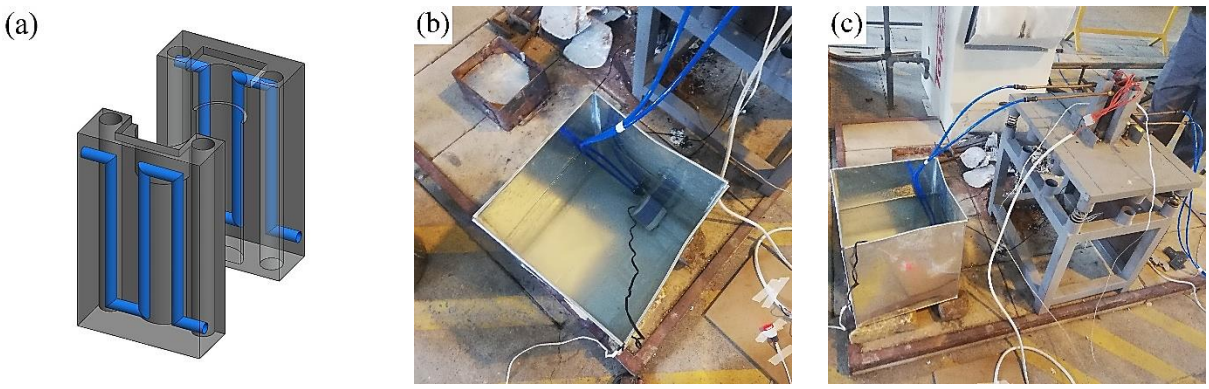

Figure 3-5: (a) CAD model of cooling channels in die (b) Cooling Tank, (c) Complete Cooling Setup

Cooling parameters are illustrated in table below.

Table 3-5: Cooling System Specifications

Parameter	**Tank Capacity**	**Flow Rate**	**Temperature In**	**Temperature Out**
Value	50 Litres	500 Ltr. /Hr.	25°C	120°C

3.5 **Process Parameters**

Experiments were designed according to Taguchi Design of Experiments. Taguchi method is an efficient problem-solving tool for design of experiments. This technique reduces significantly experimental time and cost and also improves the performance of the process, system, design and product. For the analysis of entire process parameters, Taguchi method generally employs specially designed orthogonal arrays with small number of experiments. Four input parameters are pouring temperature, die temperature, frequency and acceleration, as shown in table below.

Table 3-6: Input Parameters and Levels

Parameter	**Range**	**Level 1**	**Level 2**	**Level 3**
Pouring Temperature	700-800°C	700°C	750°C	800°C
Die Temperature	150-450°C	150°C	300°C	450°C
Frequency	15-45 Hz	15 Hz	30 Hz	45 Hz
Acceleration	0.5-1.5 g	0.5 g	1.0 g	1.5 g

The aim of our experiments was to find out the most important factor and the combination of all factors which influence to increase the mechanical properties like Ultimate tensile strength and average hardness.

This research is associated with permanent mould casting process which involves various parameters at different levels and affects the casting quality. Considering these features, Taguchi method was used to increase the ultimate tensile strength, hardness and decreasing average grain size by setting the optimum values of the design parameters of the permanent mould casting. The methodology used to achieve the optimized process parameters using Taguchi Design of Experiments is given below:

a. Select the parameters with their levels which influences the process.
b. Perform experiments with the selected parameters using Taguchi orthogonal arrays.
c. Analyze the results to get most affecting parameter and combination of all parameters.
d. Perform confirmation experiment using the best level of all influencing parameters.

To calculate number of experiments, first step is to find degrees of freedom of our experiments.

$$DOF = P\,(L - 1) \quad \text{……...……...…..……..……..…….3.7}$$

where,

DOF = Degree of Freedom
P = Number of Factors = 4
L = Number of Levels = 3

$$DOF = 4\,(3 - 1) = 8 \quad \text{……...……....…….……..…….3.8}$$

The total DOF of the orthogonal array should be equal or greater than the total DOF required for the experiment. Thus, L9 orthogonal array is selected to perform the experiments. Taguchi L9 orthogonal array formed by Minitab is illustrated in Table below.

Table 3-7: L9 Orthogonal Array

Run	**A**	**B**	**C**	**D**
1	1	1	1	1
2	1	2	2	2
3	1	3	3	3
4	2	1	2	3

5	2	2	3	1
6	2	3	1	2
7	3	1	3	2
8	3	2	1	3
9	3	3	2	1

Parameters with original level values are illustrated below in Table.

Table 3-8: Orthogonal Array with Real Values

Run	**Pouring Temperature (°C)**	**Die Temperature (°C)**	**Frequency (Hz)**	**Acceleration (g)**
1	700	150	15	0.5
2	700	300	30	1.0
3	700	450	45	1.5
4	750	150	30	1.5
5	750	300	45	0.5
6	750	450	15	1.0
7	800	150	45	1.0
8	800	300	15	1.5
9	800	450	30	0.5

3.6 **Material**

Material used in this research was hypo-eutectic Aluminum-Copper 2024 alloy. 2024 aluminum is an alloy that is often used in the aerospace industry. It has high strength-to-weight ratio and excellent fatigue resistance. Alloy solidus and liquidus temperatures are 507°C and 638°C respectively. The aluminum-copper phase diagram is shown in fig below. The eutectic point is at 33.2wt.% of copper. It can be seen from the composition that 2024 alloy lies in hypo-eutectic region. The alloy composition is given in the table below.

Table 3-9: Al-2024 Alloy Composition

Element	Al	Cu	Mg	Mn	Others
wt. %	93.2	4.4	1.3	0.6	0.5

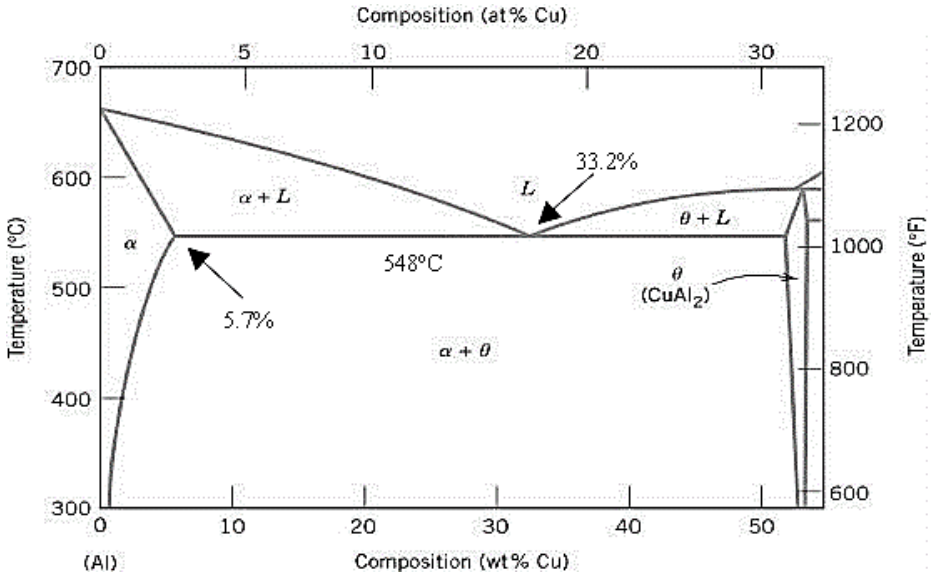

Figure 3-6: Al-Cu Phase Diagram

3.7 **Experimental Procedure**

Experimentation was carried out in Manufacturing Resource Centre, NUST. Aluminum 2024 alloy billets were melted in 'Topcast Induction Furnace'. The furnace has 45kVA power and 65 Amp current capacity. The furnace temperature was maintained 20°C above pouring temperature for compensating heat loss during pouring. The die was pre-heated to the temperature same as of the holding temperature after pouring. Metal was poured into the die using pouring cup. After pouring, vibrations were started immediately until the melt was completely solidified and die was allowed to cool down to the specified holding temperature for homogenization of grains. After holding for 10 to 15 minutes at required temperature, water pump was switched on to cool down the alloy to the room temperature to provide a faster cooling rate than air cooling. When the alloy temperature was reached to the room temperature, part was removed from the die and labelled according the taguchi array. All samples were casted with same procedure and every experiment is performed three times. One sample without vibration was also casted for comparison. Pictorial representation of the process is given below.

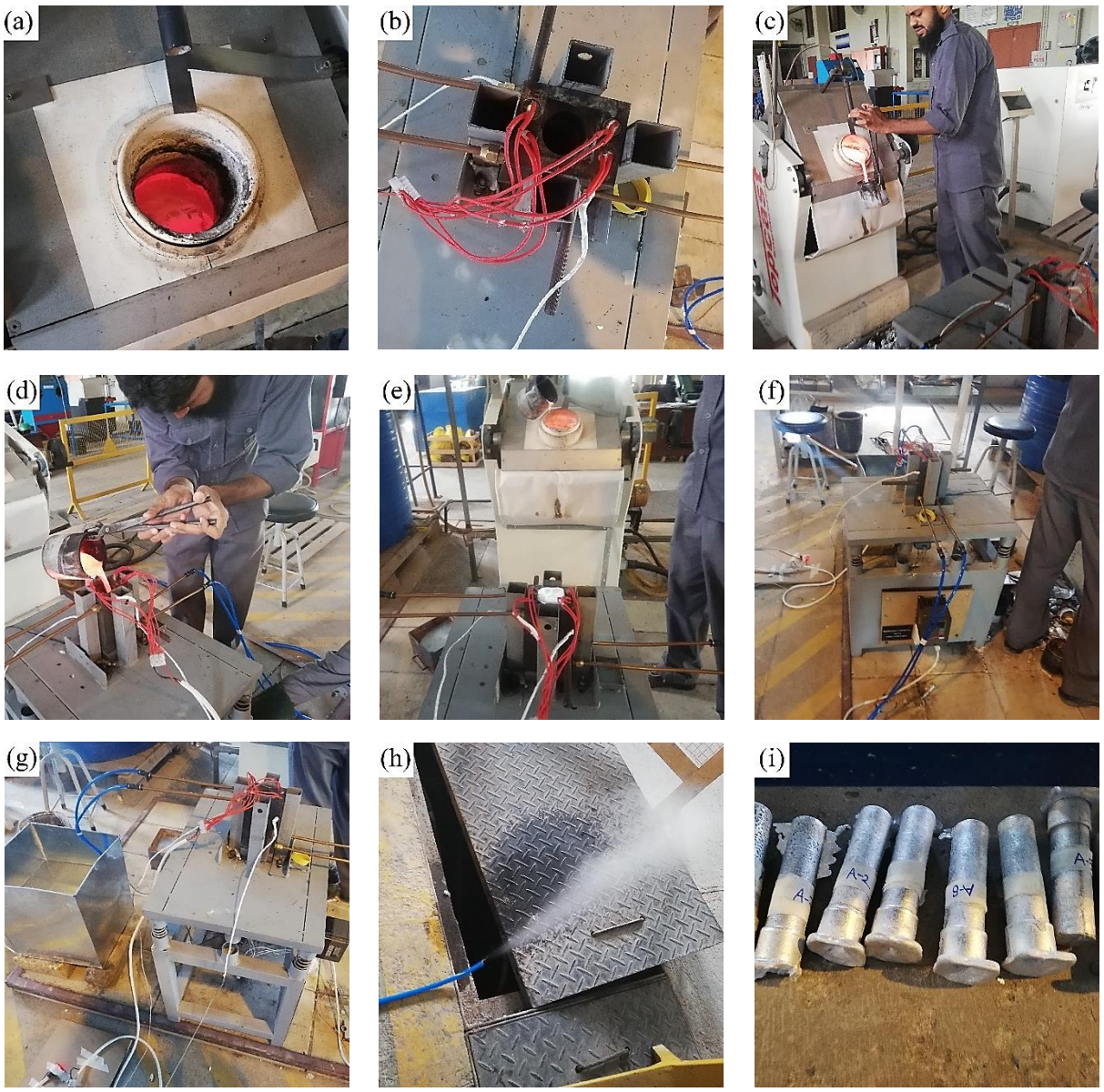

Figure 3-7: (a) Melting in Furnace, (b) Die Pre-Heating, (c) Pouring from Crucible to Pouring Cup, (d) Pouring through Pouring Cup, (e) Vibration On, (f) Vibration Stopped and Holding, (g) Water Pump on for Cooling, (h) Steam Out, (i) Casted Parts

3.8 **Heating and Cooling Curves of Mould**

Temperature of the die during casting was measured using thermocouples. Temperature vs Time readings were noted during heating and cooling. As it can be seen in figure, first the die was heated up to 150, 300 or 450 C according to the required temperature then molten metal was poured in the die. As the melt temperature was higher than the die temperature so the die temperature was raised to some degrees, during cooling when the temperature reached the required holding temperature, heaters were switched on by the automatic control system. Temperature was maintained at that point for 10 minutes and then water pump was switched on to cool down the die with an average cooling rate of 37.3°C/min.

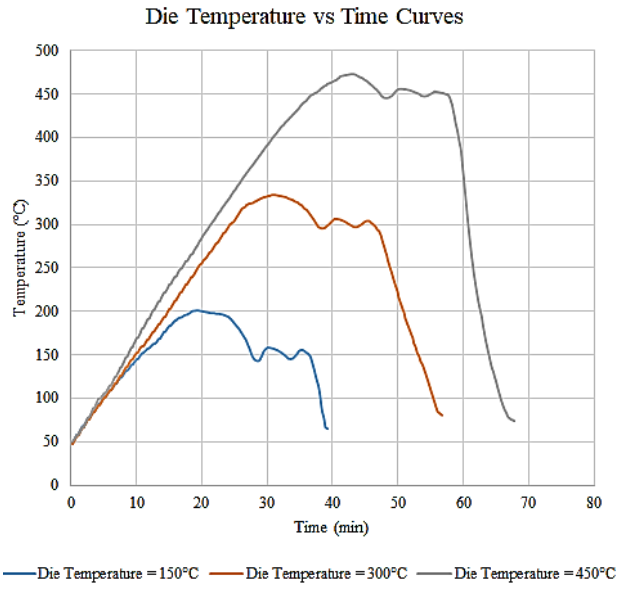

Graph 3-1: Heating and cooling temperature curves at different die temperatures

CHAPTER 4
TESTING AND SAMPLING

Two types of tests were carried out on the samples. First type is to measure the mechanical properties, like tensile strength and hardness and second type is the analysis of microstructure of the cast part.

4.1 **Tensile Test**

Samples of round dog-bone shape are used for tensile test. These samples were prepared on lathe machine according to ASTM standard E8. The working length of samples was 54 mm and diameter of neck was 9mm. For each alloy, three tensile specimens were used. Physical specimens and their dimensions are shown in figure below.

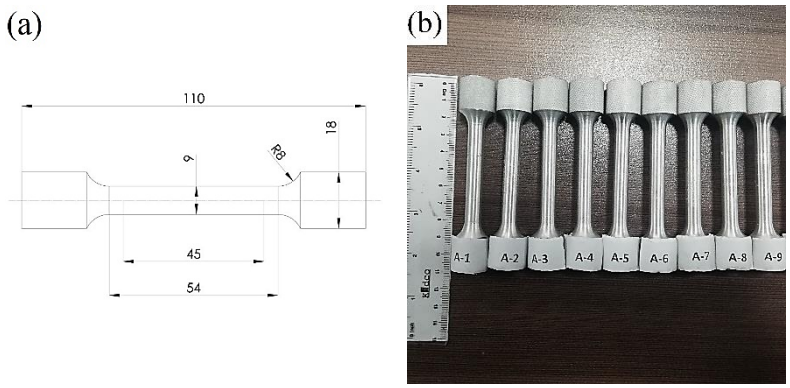

Figure 4-1: (a) Tensile test sample dimensions, (b) Physical Samples

Tensile tests were performed on ‘Shimadzu Universal Testing Machine’ by using the strain rate of 0.5 mm/mm/min. By tensile test we get proportional limit, yield stress, ultimate tensile stress, fracture point and percentage elongation. The machine used is shown in figure below.

Figure 4-2: Universal Testing Machine

4.2 **Sample Preparation for Hardness and Optical Microscopy**

Grain size was measured according to ASTM standard E112. The coin shaped samples were cut from top and bottom of cast parts using EDM wire cutting machine. All samples were first mounted on ‘Hydropress Mounting Machine’ using backlite powder. The machine is shown in figure below.

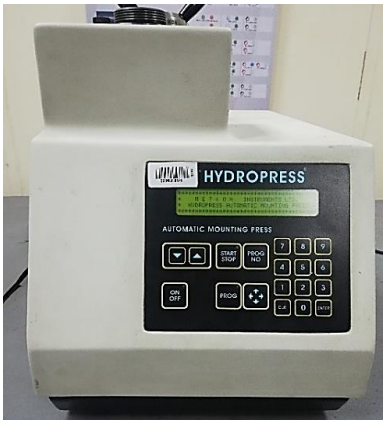

Figure 4-3: Mounting Machine

Mounted samples were then grinded on ‘Gripo 2V Manual Grinding and Polishing Machine’ using grinding papers ranging from P600 to P4000. Grinding machine is shown in figure below.

Figure 4-4: Manual Grinding Machine

The grinded samples were then polished on 1-micron polishing cloth by diamond paste on the ‘Aecotech 264 Automatic Grinding and Polishing Machine’. The machine is shown in figure below.

Figure 4-5: Automatic Polishing Machine

The Polished samples were then etched with the solution containing 25% HNO_3 and 75% distilled water. The etchant was selected from 'Metals Handbook, American Society for Metals'. For etching, the samples were immersed in solution for 45-60 seconds.

4.3 **Optical Microscopy**

After etching microstructure of the obtained casting samples were studied using 'Lumerena Optical Microscope' at 20x magnification, shown in figure 4.6 below. Micrographs were captured at three fields for every sample; one from the corner, second from the center, and third from between corner and center. The Mean Lineal Intercept method was used to measure grain size. Different Test lines were drawn with a total length L of 700um. Then number of boundaries intersected P were counted. An intersection is a point where a test line is cut by a grain boundary. The end points of a test line are not intersections and are not counted except when the end appears to exactly touch a grain boundary. A tangential intersection with a grain boundary is scored as one intersection. An intersection apparently coinciding with the junction of three grains are scored as one and a half. Then the number of 1s and 1.5s were added to get P. Then average of all fields were calculated.

$$D_{avg.} = {}^{L}/_{P} \quad \text{.....4.1}$$

where,

P = 1s + 1.5s

Figure 4-6: Optical Microscope

4.4 **Hardness**

Samples for microhardness were cut from top and bottom side of the part using EDM wire cutting machine. Micro Vickers's hardness tests were performed on 'Wolpert Group Micro Vicker Hardness Testing Machine' according to ASTM standard E384. Diamond shaped indention was made on the by applying load of 200 grams for 10 seconds on three different locations of each sample.

Figure 4-7: Micro Vicker Hardness Testing Machine

CHAPTER 5
RESULTS AND DISCUSSION

5.1 **Microstructure**

Following images are the obtained microstructures of 9-samples from top and bottom side at 20x magnification. Microstructure images taken from top of the samples are shown on the right side and images taken from bottom side of the samples are shown on the left.

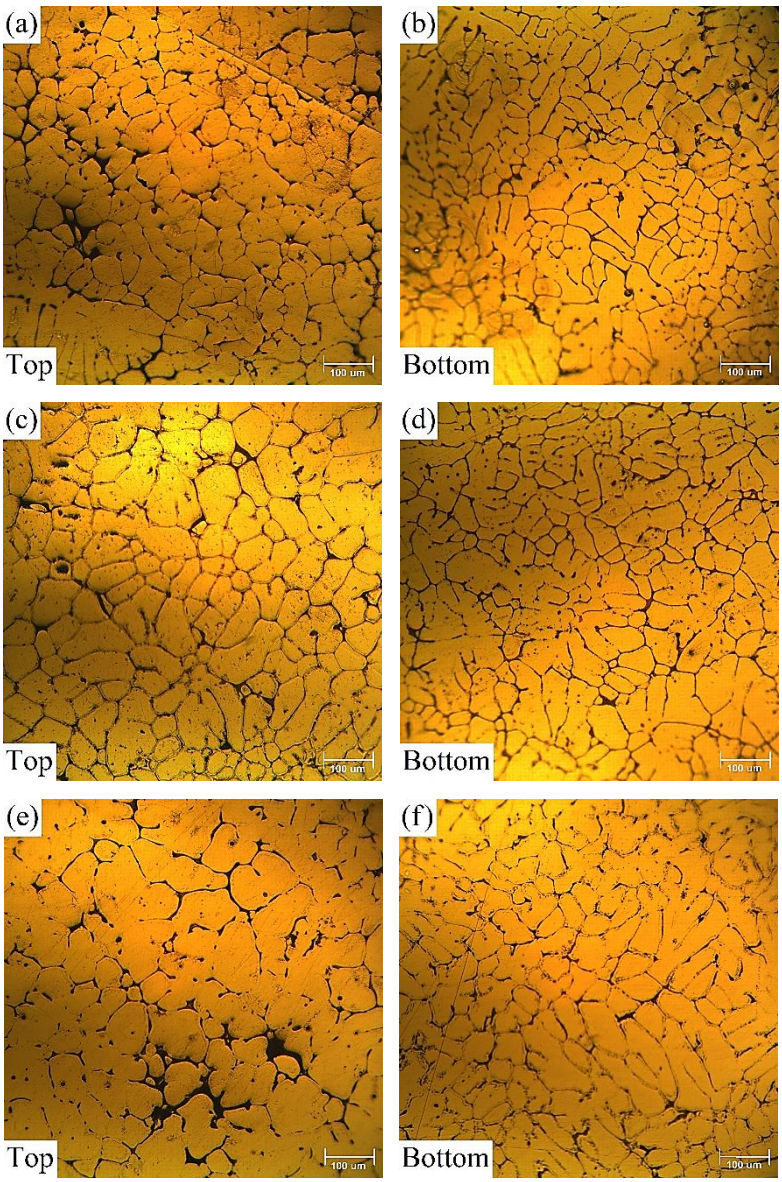

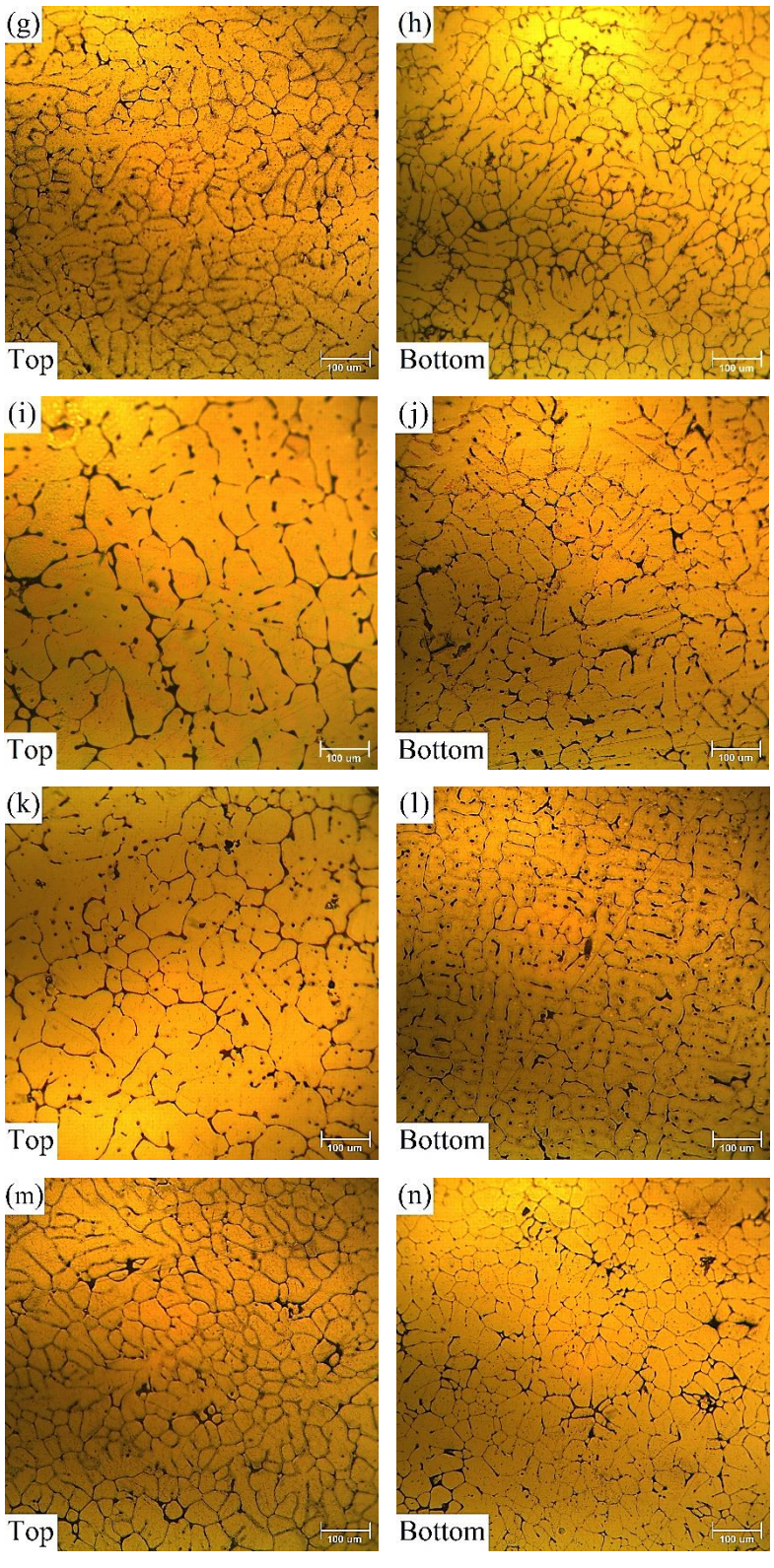
(g)
Top
100 um
(h)
Bottom
100 um
(i)
Top
100 um
(j)
Bottom
100 um
(k)
Top
100 um
(l)
Bottom
100 um
(m)
Top
100 um
(n)
Bottom
100 um

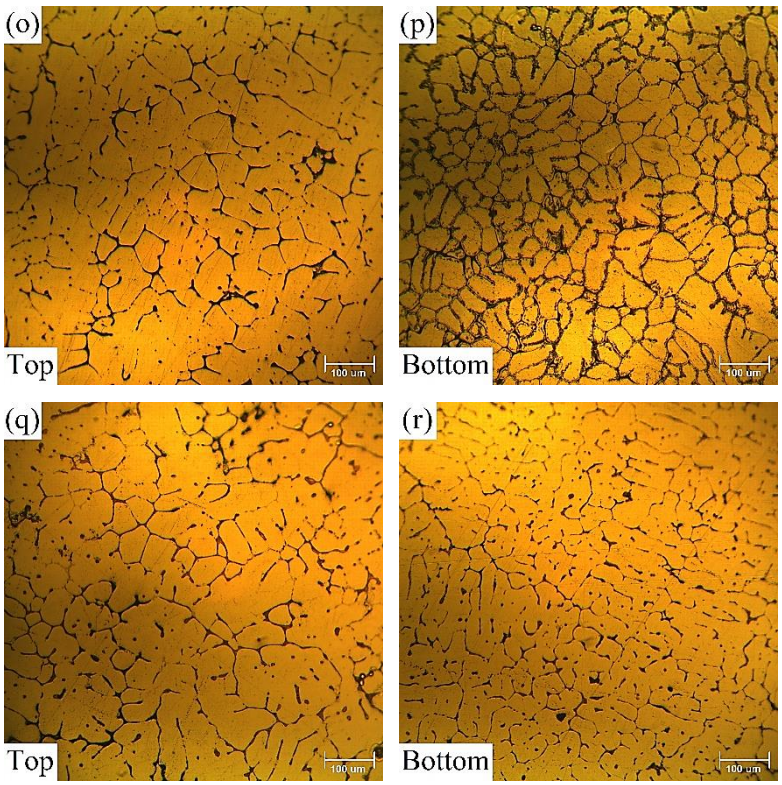

Figure 5-1: Micrographs of Run 1 to Run 9 samples from Top and Bottom sides

5.2 **Grain Size**

Table 5-1: Grain Size Results

Run	Sample Id	Grain Size (um)						Total Average
		X1		X2		X3		
		Top Avg.	Bottom Avg.	Top Avg.	Bottom Avg.	Top Avg.	Bottom Avg.	
1	A-1	31.82	26.92	30.34	27.86	33.30	25.98	**29.37**
2	A-2	35.90	32.56	36.74	31.45	35.06	33.67	**34.23**
3	A-3	46.67	43.75	47.02	42.36	46.32	45.14	**45.21**
4	A-4	34.15	25.45	33.05	24.29	34.85	27.01	**29.80**
5	A-5	60.87	35.90	59.41	40.75	58.33	35.05	**48.38**
6	A-6	58.33	27.45	43.23	39.57	53.43	35.33	**42.89**
7	A-7	25.93	24.14	23.94	23.25	28.61	24.34	**25.04**
8	A-8	51.85	36.84	49.48	39.78	54.22	33.90	**44.35**
9	A-9	32.56	32.56	31.05	29.64	35.48	34.07	**32.56**

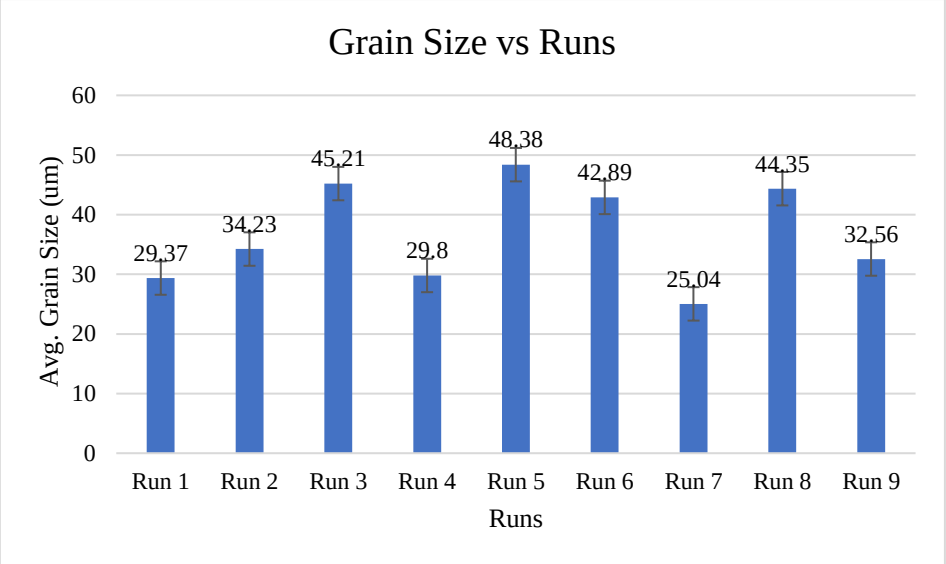

Graph 5-1: Average Grain Size vs Runs

5.3 **Hardness**

Table 5-2: Hardness Results

Run	**Sample Id**	**Vicker's Hardness (VHN)**						**Total Average**
		X1		**X2**		**X3**		
		Top Avg.	**Bottom Avg.**	**Top Avg.**	**Bottom Avg.**	**Top Avg.**	**Bottom Avg.**	
1	A-1	75.3	94.7	82.5	95.7	87.4	105.7	**90.2**
2	A-2	75.6	106.2	92.1	112.9	103.6	114.2	**100.8**
3	A-3	78.1	109.7	93.8	120.8	94.8	122.4	**103.3**
4	A-4	81.8	87	84.1	120	102.5	134.5	**101.7**
5	A-5	79.1	99.2	84.6	107.2	91.8	115.2	**96.2**
6	A-6	104.4	107.3	112.1	115.4	113.3	121.4	**112.3**
7	A-7	75.6	81.6	77	83.1	116.9	121.9	**92.7**
8	A-8	73.4	79.8	74.5	80.1	76.2	83.9	**78.0**
9	A-9	86.4	93.9	98.1	110.9	106.6	119.7	**102.6**

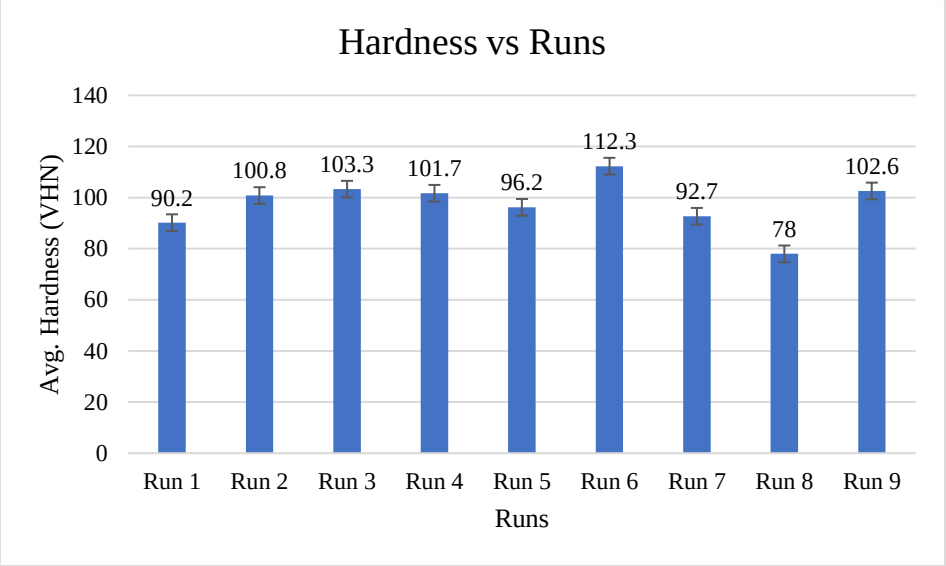

Graph 5-2: Average Hardness vs Runs

5.4 **Ultimate Tensile Strength**

Table 5-3: UTS Results

Run	**Sample Id**	**Ultimate Tensile Stress (MPA)**			
		X1	**X2**	**X3**	**Average**
1	A-1	54.3	115.2	156.6	**108.7**
2	A-2	112.7	136.5	140.5	**129.9**
3	A-3	61.3	63.7	70.5	**65.2**
4	A-4	95.7	98.4	102.6	**98.9**
5	A-5	69.0	124.9	161.3	**118.4**
6	A-6	122.5	141.7	153.1	**139.1**
7	A-7	145.8	151.4	169.5	**155.6**
8	A-8	81.4	84.2	87.5	**84.4**
9	A-9	66.6	73.8	76.4	**72.3**

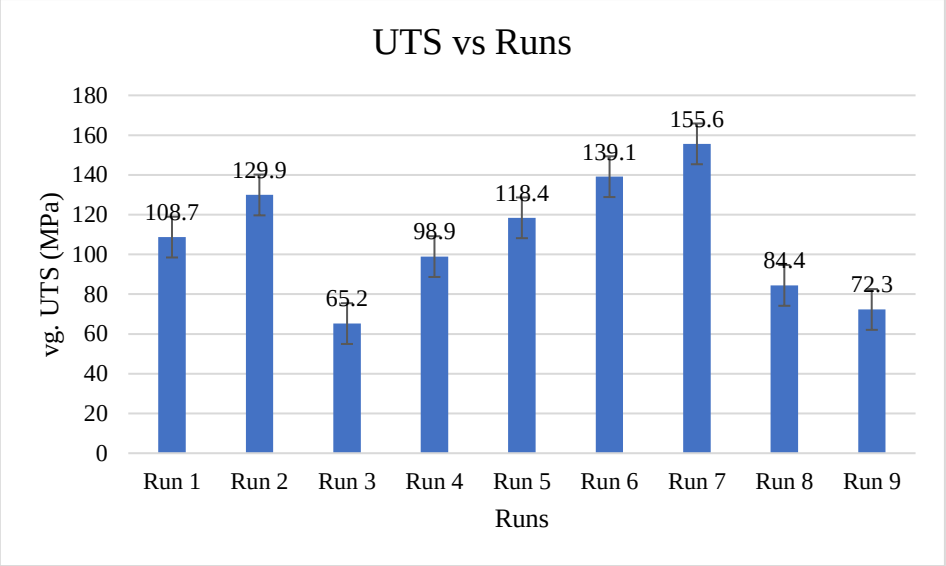

Graph 5-3: Average UTS vs Runs

5.5 **ANOVA**

The aim of our experiments was to find out the most important factor and the combination of all factors which influence to increase the mechanical properties like Ultimate tensile strength and average hardness. The experimental setup was designed on L9 orthogonal array with the of influence pouring temperature, die temperature, frequency and acceleration. Taguchi recommends that highest signal to noise ratio gives best results which can be seen from the graphs as well as from table.

This research is associated with permanent mould casting process which involves various parameters at different levels and affects the casting quality. Considering these features, Taguchi method was used to increase the ultimate tensile strength, hardness and decreasing average grain size by setting the optimum values of the design parameters of the permanent mould casting. The methodology used to achieve the optimized process parameters using Taguchi Design of Experiments is given below:

e. Select the parameters with their levels which influences the process.
f. Perform experiments with the selected parameters using Taguchi orthogonal arrays.
g. Analyze the results to get most affecting parameter and combination of all parameters.
h. Perform confirmation experiment using the best level of all influencing parameters.

The results for various combinations of processing parameters were obtained by conducting the experiments as per the Taguchi orthogonal array. Tables 5.1, 5.2 and 5.3 show the

experimental results of average repetitions for grain size measurement, hardness and tensile strength respectively. To measure the quality characteristics, the experimental values were transformed into signal to noise ratios using the commercial software MINITAB 17 which is specially used for design of experiment applications. The evaluation of results is a main step in taguchi design of experiments approach. The influence of control parameters such as pouring temperature, die temperature, frequency and acceleration has been analyzed using signal to noise response table. By Analyzing the taguchi method we can get SN ratios for each run, mean values of every parameter at each level, rank of each parameter to identify that result is sensitive to which parameter and the graphs of mean and SN ratios. Analysis of Variance gives contribution of each parameter so that we can see that which parameter affects the most to the results. Analysis of grain size, hardness and tensile strength are explained in next sections.

5.5.1 **Grain Size**

The results of different combination of factors were obtained by performing experiments according to L9 orthogonal array. The average grain size results were analyzed by Taguchi method in MINITAB-17. Signal to Noise ratio for grain size using smaller is better condition is shown in Table below.

Table 5-4: Signal to Noise Ratio for Grain Size

Run	Pouring Temperature	Die Temperature	Frequency	Acceleration	Grain Size	SNRA
1	700	150	15	0.5	29.37	-29.36
2	700	300	30	1.0	34.23	-30.69
3	700	450	45	1.5	45.21	-33.11
4	750	150	30	1.5	29.80	-28.49
5	750	300	45	0.5	48.38	-33.7
6	750	450	15	1.0	42.89	-32.65
7	800	150	45	1.0	25.04	-27.98
8	800	300	15	1.5	44.35	-32.94
9	800	450	30	0.5	32.56	-30.27

Control factors along their contribution ratios for grain size brought out by ANOVA are shown in Table 5-5 and response table for means is shown in the Table 5-6. It can be seen from the Table 5-5 that die temperature has contributed highest impact on hardness, so it is ranked one in the Table 5-6. It is concluded that the die temperature is the major contributing factor (61.74%) and frequency, pouring temperature and acceleration are second, third and fourth influencing factors respectively.

Table 5-5: Contribution, F and P Values for Grain Size

Source	DF	Seq SS	Contribution	Adj SS	Adj MS	F-Value	P-Value
Pouring Temperature	2	187.91	10.89%	187.91	93.956	61.31	0
Die Temperature	2	1065.58	61.74%	1065.58	532.791	347.66	0
Frequency	2	296.84	17.20%	296.84	148.419	96.85	0
Acceleration	2	148.04	8.58%	148.04	74.019	48.30	0
Error	18	27.59	1.60%	27.59	1.533		
Total	26	1725.96	100%				

Table 5-6: Delta and Rank for Grain Size

Level	Pouring Temperature	Die Temperature	Frequency	Acceleration
1	36.27	28.07	38.87	36.77
2	40.36	42.32	32.20	34.05
3	33.98	40.22	39.54	39.78
Delta	6.38	14.25	7.35	5.73
Rank	3	1	2	4

Response graphs are drawn from the values of Table 5-6 as shown below. By looking at these graphs one can easily understand, how the parameters affect the grain size as their value changes from one to other.

From the Graph 5-1 the optimal levels of parameters for smallest grain size are:

- Pouring Temperature at level 3 = 800°C
- Die Temperature at level 1 = 150°C
- Frequency at level 2 = 30Hz
- Acceleration at level 2 = 1.0g

Graph of Signal to Noise ratios

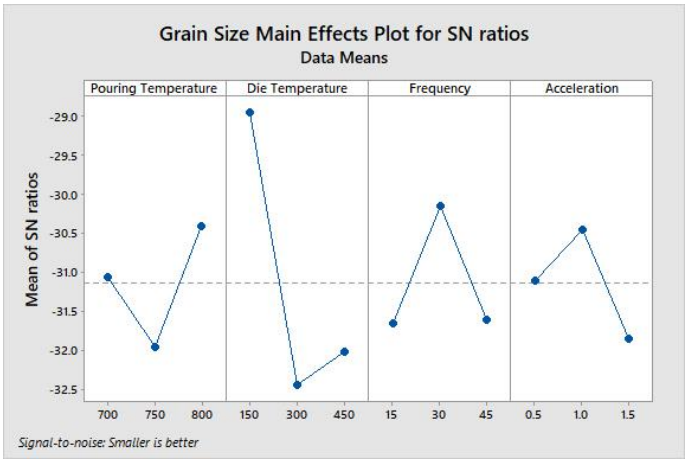

Graph 5-4: Graph of SN ratios for Grain Size

Graph of Means

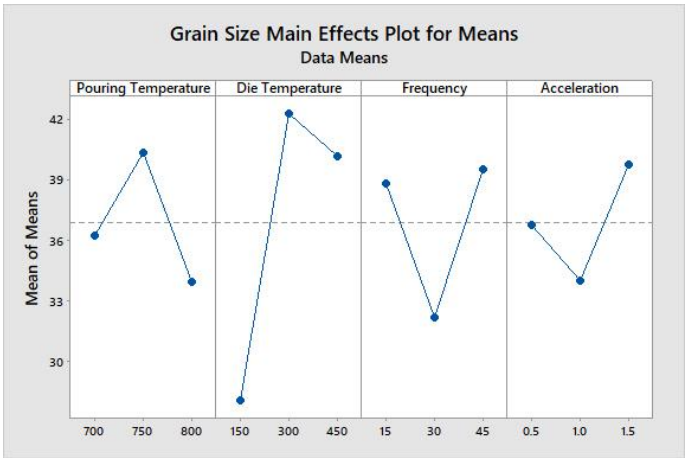

Graph 5-5: Graph of Means for Grain Size

It can be seen from the Graph 5-2 and Table 5-6 that at pouring temperature of 700°C, the average grain size was 36.27um. By increasing pouring temperature to 750°C, the average grain size increased to 40.36um. By further increasing pouring temperature to 800°C, the average grain size was decreased again to 33.98um.

It can also be seen that at die temperature of 150°C, the average grain size was 28.07um. By increasing die temperature to 300°C, the average grain size increased to 42.32um. By further increasing die temperature to 450°C, the average grain size was slightly decreased to 40.22um.

It can be also be seen that at frequency of 15Hz, the average grain size was 38.87um. By increasing frequency to 30Hz, the average grain size decreased slightly to 32.20um. By further increasing frequency to 45Hz, the average grain size was increased again to 39.54um.

It can also be seen that at acceleration of 0.5g, the average grain size was 36.77um. By increasing acceleration to 1.0g, the average grain size decreased to 34.05um. By further increasing acceleration to 1.5g, the average grain size was increased again to 39.78um.

5.5.2 **Hardness**

The results of different combination of factors were obtained by performing experiments according to L9 orthogonal array. The hardness results were analyzed by Taguchi method in MINITAB-17. Signal to Noise ratio for Hardness using larger is better condition is shown in Table below.

Table 5-7: Signal to Noise ratio for Hardness

Run	Pouring Temperature	Die Temperature	Frequency	Acceleration	Hardness	SNRA
1	700	150	15	0.5	90.2	39.105
2	700	300	30	1.0	100.8	40.042
3	700	450	45	1.5	103.3	40.269
4	750	150	30	1.5	101.7	40.104
5	750	300	45	0.5	96.2	39.648
6	750	450	15	1.0	112.3	41.002
7	800	150	45	1.0	92.7	39.252
8	800	300	15	1.5	78	37.839
9	800	450	30	0.5	102.6	40.198

Control factors along their contribution ratios for hardness brought out by ANOVA are shown in Table 5-8 and response table for means is shown in the Table 5-9. It can be seen from the

Table 5-8 that die temperature has contributed highest impact on hardness, so it is ranked one in the Table 5-9. It is concluded that the die temperature is the major contributing factor (37.65%) and pouring temperature, frequency and acceleration are second, third and fourth influencing factors respectively.

Table 5-8: Contribution, F and P Values for Hardness

Source	DF	Seq SS	Contribution	Adj SS	Adj MS	F-Value	P-Value
Pouring Temperature	2	684.5	24.99%	684.5	342.25	13.92	0
Die Temperature	2	1031.4	37.65%	1031.4	515.71	20.97	0
Frequency	2	300.4	10.97%	300.4	150.2	6.11	0.009
Acceleration	2	280.4	10.24%	280.4	140.2	5.7	0.012
Error	18	442.6	16.16%	442.6	24.59		
Total	26	2739.3	100%				

Table 5-9: Delta and Rank for Hardness

Level	Pouring Temperature	Die Temperature	Frequency	Acceleration
1	98.08	94.85	93.51	96.33
2	103.38	91.64	101.67	101.92
3	91.09	106.06	97.38	94.3
Delta	12.29	14.42	8.17	7.62
Rank	2	1	3	4

Response graphs are drawn from the values of Table 5-9 as shown below. By looking at these graphs one can easily understand, how the parameters affect the hardness as their value changes from one to other.

From the Graph 5-3 the optimal levels of parameters for highest hardness are:

- Pouring Temperature at level 2 = 750°C
- Die Temperature at level 3 = 450°C
- Frequency at level 2 = 30Hz
- Acceleration at level 2 = 1.0g

Graph of Signal to Noise ratios

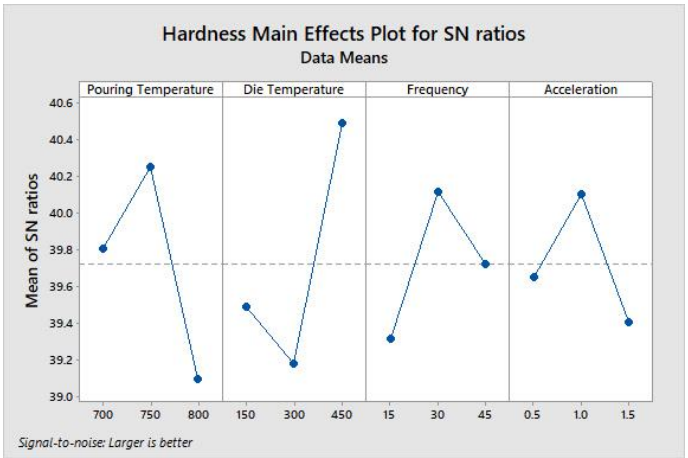

Graph 5-6: Graph of SN ratios for Hardness

Graph of Means

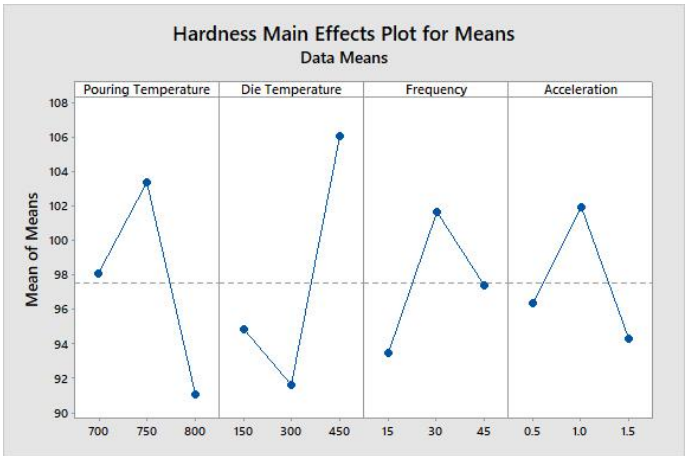

Graph 5-7: Graph of Means for Hardness

It can be seen from the Graph 5-3 and Table 5-9 that at pouring temperature of 700°C, the average hardness was 98.08VHN. By increasing pouring temperature to 750°C, the average was increased to 103.38VHN. By further increasing pouring temperature to 800°C, the average hardness was decreased to 91.09VHN.

It can be seen that at die temperature of 150°C, the average hardness was 94.85VHN. By increasing die temperature to 300°C, the average hardness decreased a little to 91.64VHN. By further increasing die temperature to 450°C, the average hardness was increased to 106.06HV.

It can also be seen that at frequency of 15Hz, the average hardness was 93.51VHN. By increasing frequency to 30Hz, the average hardness increased to 101.67VHN. By further increasing frequency to 45Hz, the average hardness was again decreased to 97.38VHN.

It can be seen that at acceleration of 0.5g, the average hardness was 96.33VHN. By increasing acceleration to 1.0g, the average hardness also increased to 101.92VHN. By further increasing acceleration to 1.5g, the average hardness was again decreased to 94.3VHN.

5.5.3 **UTS**

The results of different combination of factors were obtained by performing experiments according to L9 orthogonal array. The tensile test results were analyzed by Taguchi method in MINITAB-17. Signal to Noise ratio for UTS using larger is better condition is shown in Table below.

Table 5-10: Signal to Noise Ratio for UTS

Run	Pouring Temperature	Die Temperature	Frequency	Acceleration	UTS	SNRA
1	700	150	15	0.5	108.7	38.19
2	700	300	30	1.0	129.9	42.15
3	700	450	45	1.5	65.2	36.24
4	750	150	30	1.5	98.9	39.9
5	750	300	45	0.5	118.4	39.82
6	750	450	15	1.0	139.1	42.75
7	800	150	45	1.0	155.6	43.79
8	800	300	15	1.5	84.4	38.51
9	800	450	30	0.5	72.3	37.14

Control factors along their contribution ratios for UTS brought out by ANOVA are shown in Table 5-11 and response table for means is shown in the Table 5-12. It can be seen from the Table 5-11 that acceleration has contributed highest impact on ultimate tensile strength, so it is ranked one in the Table 5-12. It is concluded that the acceleration is the major contributing factor (48.76 %) and die temperature, pouring temperature and frequency are second, third and fourth influencing factors respectively.

Table 5-11: Contribution, F and P Values for UTS

Source	DF	Seq SS	Contribution	Adj SS	Adj MS	F-Value	P-Value
Pouring Temperature	2	1597.5	4.74%	1597.5	798.7	1.31	0.295
Die Temperature	2	3859.7	11.45%	3859.7	1929.8	3.16	0.067
Frequency	2	820.1	2.43%	820.1	410.1	0.67	0.523
Acceleration	2	16431.8	48.76%	16431.8	8215.9	13.46	0
Error	18	10990.2	32.61%	10990.2	610.6		
Total	26	33699.3	100%				

Table 5-12: Delta and Rank for UTS

Level	Pouring Temperature	Die Temperature	Frequency	Acceleration
1	101.25	121.05	110.72	99.79
2	118.80	110.89	100.36	141.53
3	104.07	92.18	113.04	82.81
Delta	17.54	28.87	12.68	58.71
Rank	3	2	4	1

Response graphs are drawn from the values of Table 5-9 as shown below. By looking at these graphs one can easily understand, how the parameters affect the tensile strength as their value changes from one to other.

From the Graph 5-5 the optimal levels of parameters for highest ultimate tensile strength are:

- Pouring Temperature at level 2 = 750°C
- Die Temperature at level 1 = 150°C
- Frequency at level 3 = 45Hz
- Acceleration at level 2 = 1.0g

Graph of Signal to Noise ratio

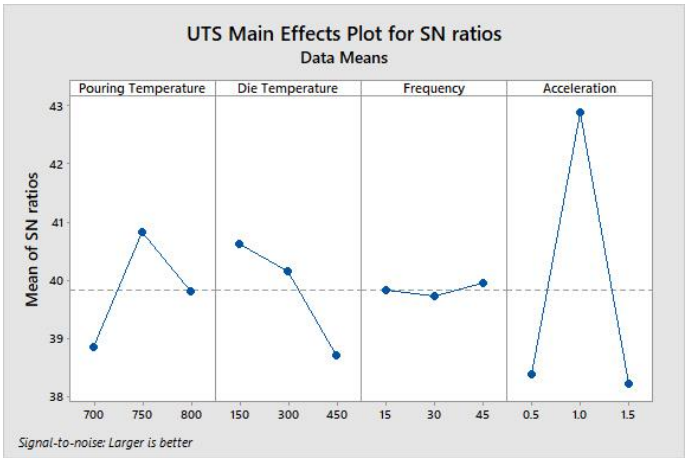

Graph 5-8: Graph of SN ratios for UTS

Graph of Means

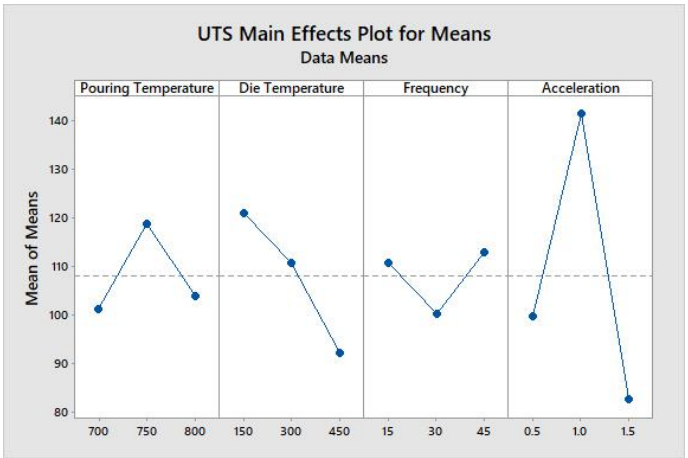

Graph 5-9: Graph of Means for UTS

It can be seen from Graph 5-5 and Table 5-12 that at pouring temperature of 700°C, the ultimate tensile strength was 101.25MPa. By increasing pouring temperature to 750°C, the ultimate tensile strength was increased to 118.80MPa. By further increasing pouring temperature to 800°C, the average ultimate tensile strength was decreased to 104.07MPa.

It can be seen that at die temperature of 150°C, the tensile strength was 121.05MPa. By increasing die temperature to 300°C, the tensile strength decreased to 110.89MPa. By further increasing die temperature to 450°C, the tensile strength was also decreased to 92.18MPa.

It can also be seen that at frequency of 15Hz, tensile strength was 110.72MPa. By increasing frequency to 30Hz, the tensile strength decreased to 100.36MPa. By further increasing frequency to 45Hz, the tensile strength was increased to 113.04MPa.

It can be seen that at acceleration of 0.5g, the tensile strength was 99.79MPa. By increasing acceleration to 1.0g, the tensile strength increased to 141.53MPa. By further increasing acceleration to 1.5g, the tensile strength was much decreased to 82.81MPa.

The methodology described above based on process knowledge was manifested through modeling work using Taguchi's Design of Experiment by MINITAB software. Four process parameters with three levels of values were practically analyzed. The process parameters namely pouring temperature, die temperature, frequency and acceleration were used to yield the result for analysis.

5.6 Confirmation Experiment and Comparison with As-Cast

A confirmation experiment was performed at the optimum settings of the process parameters for both ultimate tensile strength and hardness recommended by MINITAB by analyzing Taguchi design at larger is better signal to noise ratio setting.

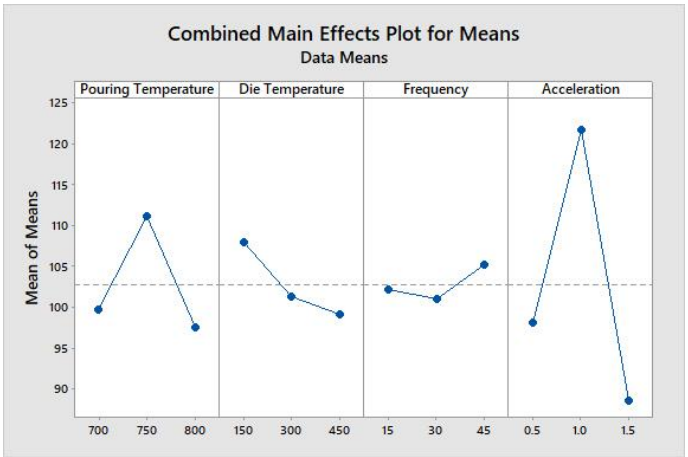

Graph 5-10: Graph of Means for Combined effect of hardness and UTS

As seen from the graph, optimum values are those which have highest mean values i-e 750°C pouring temperature, 150°C die temperature, 45Hz frequency and 1.0g of acceleration. So, the

confirmation experiment was carried out at these parameter values which are also shown in Table below.

Table 5-13: Optimum Parameter Values

Pouring Temperature	Die Temperature	Frequency	Acceleration
750°C	150°C	45Hz	1.0g

Microstructures of confirmation experiment performed at optimum parameter conditions and as-cast samples are shown in figure below. It can be seen that in as-cast microstructure the grains are coarse and dendrites are present and some rosette like coarse dendrites are also present. Whereas, in confirmation experiment small globular grains and at some places irregular shaped grains are also present. So, we can say that vibration has a positive impact on grain structure.

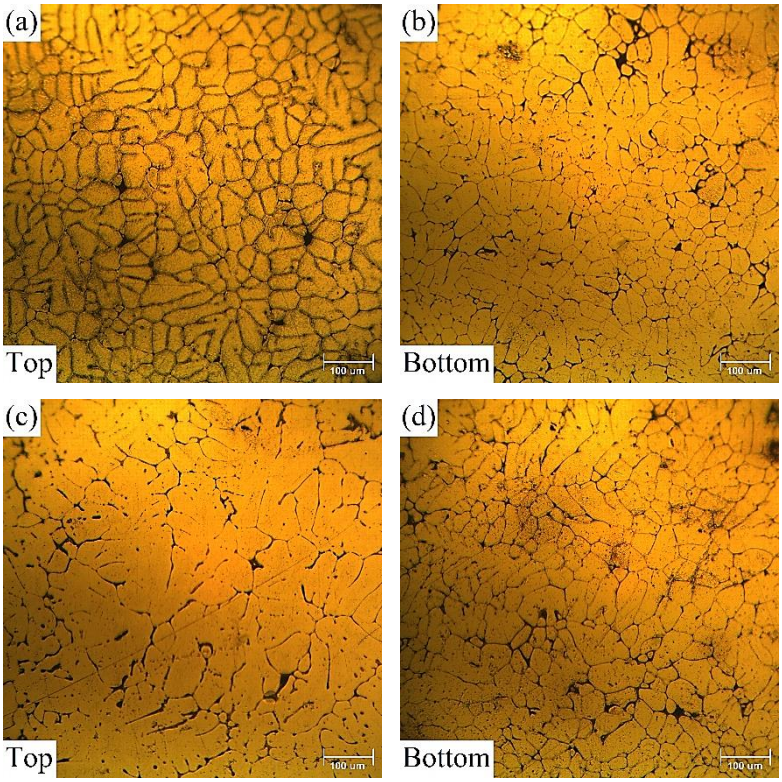

Figure 5-2: Optical Micrographs of (a) Top Side, (b) Bottom Side of Confirmation Experiment, (c) Top Side, (d) Bottom Side of As-cast

Table 5-14: Results of Confirmation Experiment and As-cast

Property / Experiment	Grain Size (um)			Hardness (VHN)			UTS (MPa)
	Top	Bottom	Avg.	Top	Bottom	Avg.	
Optimum	25.45	23.73	**24.59**	106.3	113.5	**109.9**	**161.3**
As-Cast	48.26	35.00	**41.64**	92.8	100.7	**96.8**	**145.9**

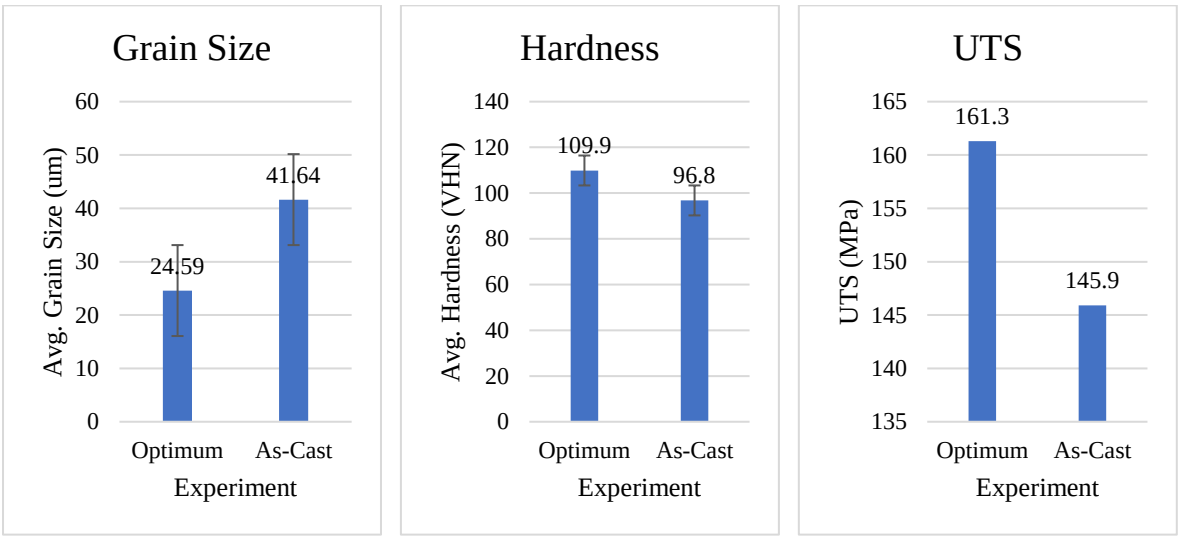

Graph 5-11: Comparison of Grain Size, Hardness and UTS of Optimum and As-Cast Experiments

The average grain size obtained at these settings was 24.59um which was decreased by 40.9% as compared to as-cast sample. The UTS and hardness values obtained at these optimum settings were 161.3 MPa and 109.9VHN which were increased by 10.6% and 13.5% respectively.

5.7 **Discussion**

5.7.1 **Grain Size**

Introducing vibration to the melt decreased the effect of pouring temperature and prevented the coarse grains to form. When pouring temperature was increased, it decreased the solidification rate which caused coarse grains to form. But with the increase in vibration intensity, air gap between the mould wall and the sample was reduced, which increased the rate of heat transfer, thus reduced the effect of high pouring temperature. As a result, fine structures were obtained due to increased heat transfer and high cooling rate which occurred due to elimination of air gaps [18].

In as-cast case, bottom side of casting had a fine structure as compared to top. This happened due to high conductivity of mould. As the bottom side of the mould was attached to the body whereas the top side was open to atmosphere, so heat transfer rate was more in lower portion than the top according to laws of heat transfer [6]. In the case of vibration, die was pre heated to specified temperature. When the metal was poured into the die and held at that temperature for 10 minutes, the temperature throughout the part was almost uniform, as a result the difference between grains at top and bottom was reduced.

At 15Hz, due to alternate movement of the liquid, heat transfer rate was increased and hence higher cooling rate. At 30Hz, the vibration induced even more cooling rate due to forced convection and solidification time was further reduced. At 45Hz, the vibrations must had induced even more cooling rate due to very rapid movement of melt. However, a loss of contact was created between liquid-mould interface due to higher relative acceleration, as a result conductive heat transfer was converted into conductive + convective. As result coarser microstructure was obtained which means low mechanical properties [9].

At 0.5g acceleration, due to frequent movement of melt, coarse grains were refined to some extent. At 1.0g, due to higher movement and rotation of grains and high convection rate, temperature was uniformly distributed in all directions. Higher cooling rates were obtained due to vigorous convection and high heat transfer. Therefore, grain multiplication, more nucleation, and higher grain refinement. When the applied acceleration was 1.5g, the grains and rosette like dendrites of α-Al had been fractured under exciting force. Excessive mechanical acceleration had caused defects such as porosity, casting loose and poor formability [8].

5.7.2 **Hardness**

Cooling rate increases by reducing the casting temperature. The higher hardness for dynamically casted samples at 750°C can be attributed to the high cooling rate, fine grains and the reduction of the porosity content [18]. At 800°C, the hardness was decreased due to long freezing time which was caused by lower cooling rate during solidification. Slow cooling softens the material as like in annealing [10].

The samples casted at 450°C die temperature had shown higher hardness. This can be explained as water cooling was started from higher temperatures, so due to increased cooling rate caused by quenching effect, these samples show higher hardness as compared to samples casted at 300°C and 150°C [10].

The hardness is also increasing as the frequency has been increased. Maximum hardness is at frequency 30 Hz. This could be explained that the structures of the Al alloys consist of a solid solution and the (β phase) compound intermetallic at the grain boundaries as the phase solidifying last. The compound fills inter-dendritic cavities and thus influences flowability, shrinkage, porosity, and the development of cracks. The hardness of the alloys depends on the character of the intermetallic phases [5].

It is clear that hardness of casting increases with the increase in vibration acceleration because vibration causes refinement of grains. So, we may conclude that due to combined effect of cooling rate and intensity of vibration, there are remarkable changes of hardness in the cast product [6]. It is conspicuously revealed that the hardness of samples increases with the increase in vibration acceleration, reaches the maximum at 1.0g and then begins to fall due to porosity caused by excessive acceleration [7].

5.7.3 **Ultimate Tensile Strength**

According to Hall and Petch relationship grain size is inversely proportional to mechanical properties i-e finer the microstructure, higher are the mechanical properties and vice versa. Harder materials are strong due to their smaller grain size. Vibration makes material brittle and reduces its elongation and hence ductility [13].

When the die was pre heated at 150°C, due to large temperature difference between mould wall and the liquid, the alloy, cooling rate was increased. The lower solidification times caused fine microstructure. Due to smaller grains, more grain boundaries were formed which made samples stronger than other samples casted at different die temperatures [10].

When the acceleration was increased from 0.5g to 1.0g, average α-Al grain size decreased and tensile strength of the alloy increased significantly. The porosity under these accelerations was lower than that without vibration. This may be caused by the breakage of dendrites and effective feeding. At 1.5g, α-Al grains should be decreased even more, but due to strong vibration, small air bubbles migrated and gathered together a big bubble surface, near the solidifying grains, eventually forming a large spherical pore. The migrating, gathering and growth of bubbles led to the growth of pores which eventually decreased the tensile strength [13].

The high porosity microstructure observed in Run 3, which was subjected to the vibration treatment by 45Hz and 1.5g, is a result of applying too high of a vibration. The obtained

microstructure with high differences in density of the alloy is the result of the segregation effect during metal solidification. As a result, the high porosity of the alloy is the main reason for the inability to determine its mechanical properties [2].

There was no significant change observed on UTS by changing pouring temperature and Frequency.

CHAPTER 6
CONCLUSIONS AND FUTURE WORKS

6.1 **Conclusions**

We can conclude that by the application of mechanical vibrations in semi-solid state of Aluminum 2024 alloy showed remarkable effects on the microstructure and mechanical properties. Following conclusions can be drawn from this research work:

- Taguchi Design of Experiment approach was used in this thesis which helped a lot in the sense of reducing number of experiments without losing the confidence level. By this approach our experiments were reduced from 81 to only 9, which saved our time, cost and effort.
- Average grain size of the parts was decreased and a non-dendritic microstructure with fine globular grains were obtained by using vibration treatment.
- Mechanical properties like tensile strength and hardness increased till a certain level of vibration intensity (frequency, acceleration) but decreased with higher levels.
- Best results were achieved at medium pouring temperature (750°C), lowest die temperature (150°C), highest frequency (45Hz) and medium acceleration (1.0g).
- The average grain size obtained at the optimum settings was 24.59um which was decreased by 40.9% as compared to as-cast sample. The UTS and hardness values obtained at these optimum settings were 161.3 MPa and 109.9VHN which were increased by 10.6% and 13.5% respectively.
- There was a difference observed in the grains and hardness of the top and bottom side of the as-cast sample. Vibration and holding had reduced the difference in values of average grain size and hardness between top and bottom side. In as-cast situation the average grain size at the bottom of the part was 27.5% smaller than the top, whereas in confirmation experiment this difference was reduced to 6.7%. The average hardness of as-cast sample at the bottom was 8.5% greater than the top, whereas this difference was reduced to 6.8% in confirmation experiment.
- In most cases a dense microstructure was obtained and the parts were free from casting defects like shrinkage cavities and porosity. Porosity was observed only in the part casted at highest frequency and acceleration values i-e 45Hz and 1.5g.

6.2 **Future Works**

On the basis of research conducted, following future works are suggested:

a. Combined effect of Dynamic Solidification and Rheo-Casting may be considered.
b. Heat treatment such as Solid Solution Treatment and Aging effects may be used.
c. Ultrasonic vibration treatment before pouring may be used
d. Cooling slope casting may be used coupled with dynamic solidification.
e. Vibrating probes may be used for producing vibrations.

CHAPTER 7
REFERENCES

[1] C. Limmaneevichitr, S. Pongananpanya, and J. Kajornchaiyakul, "Metallurgical structure of A356 aluminum alloy solidified under mechanical vibration: An investigation of alternative semi-solid casting routes," *Mater. Des.*, vol. 30, no. 9, pp. 3925–3930, 2009, doi: 10.1016/j.matdes.2009.01.036.

[2] V. Selivorstov, Y. Dotsenko, and K. Borodianskiy, "Influence of low-frequency vibration and modification on solidification and mechanical properties of Al-Si casting alloy," *Materials (Basel).*, vol. 10, no. 5, pp. 1–15, 2017, doi: 10.3390/ma10050560.

[3] P. Appendino *et al.*, "SAND-CAST ALUMINIUM ALLOYS," pp. 27–32.

[4] H. M. Guo, A. S. Zhang, X. J. Yang, and M. M. Yan, "Grain refinement of Al-5%Cu aluminum alloy under mechanical vibration using meltable vibrating probe," *Oral Oncol.*, vol. 50, no. 10, pp. 2489–2496, 2014, doi: 10.1016/S1003-6326(14)63375-6.

[5] V. Chaturvedi and U. Pandel, "STUDY OF MECHANICAL VIBRATION ON STRUCTURE AND PROPERTIES OF Mg-9Al ALLOY DURING SOLIDIFICATION," *Int. Conf. Appl. Mech. Mech. Eng.*, vol. 17, no. 17, pp. 1–7, 2016, doi: 10.21608/amme.2016.35174.

[6] S. S. Mishra, S. S. Sahu, and V. Ray, "Effect of Mold Vibration on Mechanical and Metallurgical Properties of Al-Cu Alloy," vol. 3, no. 1, pp. 131–134, 2015.

[7] A. Fatai Olufemi and I. Simeon Ademola, "Effects of Melt Vibration During Solidification on the Mechanical Property of Mg-Al-Zn Alloy," *Int. J. Metall. Eng.*, vol. 1, no. 3, pp. 40–43, 2012, doi: 10.5923/j.ijmee.20120103.02.

[8] J. Chen, X. Chen, and Z. Luo, "Effect of mechanical vibration on microstructure and properties of cast AZ91D alloy," *Results Phys.*, vol. 11, no. October, pp. 1022–1027, 2018, doi: 10.1016/j.rinp.2018.10.047.

[9] G. Chirita, I. Stefanescu, D. Soares, and F. S. Silva, "Influence of vibration on the solidification behaviour and tensile properties of an Al-18 wt%Si alloy," *Mater. Des.*, vol. 30, no. 5, pp. 1575–1580, 2009, doi: 10.1016/j.matdes.2008.07.045.

[10] P. S. Kumar, E. Abhilash, and M. A. Joseph, "Solidification under Mechanical

Vibration: Variation in Metallurgical Structure of Gravity Die Cast A356 Aluminium Alloy," *Int. Conf. Front. Mech. Eng. (FIME 2010)*, no. December 2015, pp. 140–146, 2010.

[11] S. Gencalp and N. Saklakoglu, "Effects of Low-Frequency Mechanical Vibration and Casting Temperatures on Microstructure of Semisolid AlSi8Cu3Fe Alloy," *Arab. J. Sci. Eng.*, vol. 37, no. 8, pp. 2255–2267, 2012, doi: 10.1007/s13369-012-0316-0.

[12] V. V. Promakhov, M. G. Khmeleva, I. A. Zhukov, V. V. Platov, A. P. Khrustalyov, and A. B. Vorozhtsov, "Influence of vibration treatment and modification of A356 aluminum alloy on its structure and mechanical properties," *Metals (Basel).*, vol. 9, no. 1, 2019, doi: 10.3390/met9010087.

[13] Z. Zhao, Z. Fan, X. Dong, B. Tang, D. Pan, and J. Li, "Influence of mechanical vibration on the solidification of a lost foam cast 356 alloy," *China Foundry*, vol. 7, no. 1, pp. 24–29, 2010.

[14] G. N. Sahadeva, A. S. Ravindran, T. Chandrashaker, and H. R. Vitala, "Influence of Ultrasonic Vibrations on Grain Size and Mechanical Properties of A-356 by Adding Al-5Ti-1B Master Alloy during Solidification," vol. 5, no. 10, pp. 1–10, 2015.

[15] S. Mishra, M. Saleem, R. Kumar, and Amitesh, "Effect of Mould Vibration on Microstructure and Mechanical Properties of Casting During Solidification - a," *Ijert*, vol. 5, no. March, pp. 11–13, 2016.

[16] Y. Zhao, W. Zhang, F. Meng, Z. Wang, D. Zhang, and C. Yang, "Microstructure and Mechanical Properties of as-Cast Al-5.0Cu-0.6Mn-0.6Fe Alloy Produced by Ultrasonic Vibration and Applied Pressure," *Xiyou Jinshu Cailiao Yu Gongcheng/Rare Met. Mater. Eng.*, vol. 47, no. 2, pp. 457–462, 2018, doi: 10.1016/s1875-5372(18)30088-2.

[17] K. Arul, T. Manoj, A. Thanikasalam, and J. Elanchezh, "Investigation of Squeeze Casting on Metal Matrix Composite [Al-Sic (P) Reinforced," *Int. J. Adv. Eng. Res. Dev.*, vol. 2, no. 03, pp. 390–396, 2015, doi: 10.21090/ijaerd.020366.

[18] A. Jahangiri, S. P. H. Marashi, M. Mohammadaliha, and V. Ashofte, "The effect of pressure and pouring temperature on the porosity, microstructure, hardness and yield stress of AA2024 aluminum alloy during the squeeze casting process," *J. Mater. Process. Technol.*, vol. 245, pp. 1–6, 2017, doi: 10.1016/j.jmatprotec.2017.02.005.

[19] E. Hajjari and M. Divandari, “An investigation on the microstructure and tensile properties of direct squeeze cast and gravity die cast 2024 wrought Al alloy,” *Mater. Des.*, vol. 29, no. 9, pp. 1685–1689, 2008, doi: 10.1016/j.matdes.2008.04.012.

[20] M. Dhanashekar and V. S. Senthil Kumar, “Squeeze casting of aluminium metal matrix composites - An overview,” *Procedia Eng.*, vol. 97, pp. 412–420, 2014, doi: 10.1016/j.proeng.2014.12.265.

[21] B. Vanko, L. Stanček, and R. Moravčík, “EN AW-2024 wrought aluminum alloy processed by casting with crystallization under pressure,” *Stroj. Cas.*, vol. 67, no. 2, pp. 109–116, 2017, doi: 10.1515/scjme-2017-0024.

[22] Y. Li, Y. Li, C. Li, and H. Wu, “Microstructure characteristics and solidification behavior of wrought aluminum alloy 2024 rheo-diecast with self-inoculation method,” *China Foundry*, vol. 9, no. 4, pp. 328–336, 2012.

[23] G. Chen *et al.*, “Ultrasonic assisted squeeze casting of a wrought aluminum alloy,” *J. Mater. Process. Technol.*, vol. 266, no. October 2018, pp. 19–25, 2019, doi: 10.1016/j.jmatprotec.2018.10.032.

[24] G. Chen *et al.*, “Microstructures and mechanical properties of in-situ Al3Ti/2024Al composites after solution and subsequent aging treatment,” *Mater. Sci. Eng. A*, vol. 724, no. February, pp. 181–188, 2018, doi: 10.1016/j.msea.2018.03.089.

[25] J. Leng, G. Wu, Q. Zhou, Z. Dou, and X. L. Huang, “Mechanical properties of SiC/Gr/Al composites fabricated by squeeze casting technology,” *Scr. Mater.*, vol. 59, no. 6, pp. 619–622, 2008, doi: 10.1016/j.scriptamat.2008.05.018.

[26] J. W. Kaczmar, K. Naplocha, and J. Morgiel, “Microstructure and strength of Al2O3 and carbon fiber reinforced 2024 aluminum alloy composites,” *J. Mater. Eng. Perform.*, vol. 23, no. 8, pp. 2801–2808, 2014, doi: 10.1007/s11665-014-1036-2.

[27] R. N. Rao and S. Das, “Effect of applied pressure on the tribological behaviour of SiCp reinforced AA2024 alloy,” *Tribol. Int.*, vol. 44, no. 4, pp. 454–462, 2011, doi: 10.1016/j.triboint.2010.11.018.

[28] X. Kai, K. Tian, C. Wang, L. Jiao, G. Chen, and Y. Zhao, “Effects of ultrasonic vibration on the microstructure and tensile properties of the nano ZrB2/2024Al composites

synthesized by direct melt reaction," *J. Alloys Compd.*, vol. 668, pp. 121–127, 2016, doi: 10.1016/j.jallcom.2016.01.152.

[29] L. Zhang, W. Li, and J. P. Yao, "Microstructures and thermal stability of the semi-solid 2024 aluminum alloy prepared using the pulsed magnetic field process: Effects of technological parameters," *J. Alloys Compd.*, vol. 554, pp. 156–161, 2013, doi: 10.1016/j.jallcom.2012.10.185.

[30] H. M. Guo and X. J. Yang, "Rheoforging of wrought aluminum alloys," *Solid State Phenom.*, vol. 141–143, pp. 271–276, 2008, doi: 10.4028/www.scientific.net/ssp.141-143.271.